Cerebral Cortex May 2012;22:1052-1067
doi:10.1093/cercor/bhr178
Advance Access publication July 17, 2011

Neural Correlates of Perceptual Decision Making before, during, and after Decision Commitment in Monkey Frontal Eye Field

Long Ding and Joshua I. Gold

Department of Neuroscience, University of Pennsylvania, Philadelphia, PA 19104-6074, USA

Address correspondence to Long Ding, Department of Neuroscience, 117 Johnson Pavilion, 3610 Hamilton Walk, University of Pennsylvania, Philadelphia, PA 19104-6074, USA. Email: lding@mail.med.upenn.edu.

Perceptual decision making requires a complex set of computations to implement, evaluate, and adjust the conversion of sensory input into a categorical judgment. Little is known about how the specific underlying computations are distributed across and within different brain regions. Using a reaction-time (RT) motion direction-discrimination task, we show that a unique combination of decision-related signals is represented in monkey frontal eye field (FEF). Some responses were modulated by choice, motion strength, and RT, consistent with a temporal accumulation of sensory evidence. These responses converged to a threshold level prior to behavioral responses, reflecting decision commitment. Other responses continued to be modulated by motion strength even after decision commitment, possibly providing a memory trace to help evaluate and adjust the decision process with respect to rewarding outcomes. Both response types were encoded by FEF neurons with both narrow- and broad-spike waveforms, presumably corresponding to inhibitory interneurons and excitatory pyramidal neurons, respectively, and with diverse visual, visuomotor, and motor properties, albeit with different frequencies. Thus, neurons throughout FEF appear to make multiple contributions to decision making that only partially overlap with contributions from other brain regions. These results help to constrain how networks of brain regions interact to generate perceptual decisions.

Keywords: motion discrimination, nonhuman primate, oculomotor, prefrontal cortex, saccade

Introduction

Many perceptual decisions require the brain to accumulate incoming sensory evidence gradually over time. For a decision about the direction of random-dot motion that leads to an eye-movement response (DOTS task; Newsome et al. 1989), this accumulation process is encoded by certain neurons in parts of the prefrontal cortex (PFC) including the frontal eye field (FEF), the lateral intraparietal area (LIP), and two of their subcortical targets, the caudate nucleus in the basal ganglia and the superior colliculus (SC) (Shadlen and Newsome 1996; Horwitz and Newsome 1999; Kim and Shadlen 1999; Roitman and Shadlen 2002; Ding and Gold 2010). However, the resulting accumulated quantity can have multiple uses, including determining the current choice and persisting beyond the current choice to drive expectations and learning. It is not yet understood how these multiple uses are encoded within and across these brain regions. We used a reaction-time (RT) version of the DOTS task, which has already been used to characterize responses in LIP and caudate, to examine how neurons in FEF with different response properties relate to these different decision-related functions.

We targeted the FEF because its anatomical and functional properties suggest that it might play multiple roles in decision making. The FEF is reciprocally connected to area LIP and, like LIP, receives visual-motion inputs and projects to both SC and caudate (Kemp and Powell 1970; Goldman and Nauta 1977; Kunzle and Akert 1977; Yeterian and Van Hoesen 1978; Schiller et al. 1979; Maunsell and van Essen 1983; Boussaoud et al. 1990; Felleman and Van Essen 1991; Schall, Morel, et al. 1995). Neural activity in the FEF encodes numerous aspects of saccade processing, including target identification in visual-search tasks (Thompson et al. 1996; Bichot and Schall 1999, 2002; Bichot, Thompson, et al. 2001; Sato and Schall 2003; Cohen, Heitz, et al. 2009; Monosov et al. 2010), flexible decision criteria in a motion speed-discrimination task (Ferrera et al. 2009), saccade commitment (Hanes and Schall 1996; Woodman et al. 2008), and internally generated error signals (Ferrera and Barborica 2010). Some FEF activity is modulated by more general cognitive signals that can influence decision making, such as attention and reward expectation (Coe et al. 2002; Roesch and Olson 2003; Ding and Hikosaka 2006; Monosov and Thompson 2009; Zhou and Thompson 2009). Consistent with these response properties, suprathreshold electrical stimulation of FEF evokes saccades with a short latency (Robinson and Fuchs 1969) and subthreshold stimulation can influence spatial attention and saccade selection (Burman and Bruce 1997; Moore and Fallah 2001; Moore and Armstrong 2003).

These multiple roles in decision making might involve different subsets of neurons within FEF, which contains a variety of neurons that have typically been categorized in 2 ways. First, responses on a memory-guided saccade (MGS) task have been used to divide FEF neurons into visual, visuomovement, and movement categories (Bruce and Goldberg 1985). Of these, only a subset of neurons have been examined extensively with respect to decision-related firing properties (Kim and Shadlen 1999). Second, spike rate and waveform shape can be used to distinguish excitatory pyramidal neurons from γ-aminobutyric acid (GABA)-ergic inhibitory interneurons (Wilson et al. 1994). This distinction has been used extensively in the construction of computational models that show how certain neural networks can implement decision-related computations but without direct experimental data (Wang 2002; Beck et al. 2008; Grossberg and Pilly 2008).

Here, we show that the responses of individual FEF neurons in monkeys performing the RT DOTS task are consistent with multiple roles in decision formation. Some neurons encode the process of accumulating evidence to a decision bound, like in LIP. Other neurons continue to encode properties of the stimulus even after the decision, possibly to predict and evaluate the outcome, like in caudate. Both types of activity are found in FEF neurons of different categories, with quantitative differences in

their prevalence and timing. These results help provide important constraints on our understanding of how the computations needed to form decisions are implemented by circuits of neurons within and across different brain regions.

Materials and Methods

We used 2 adult male rhesus monkeys (*Macaca mulatta*), both of which were used in a previous study of caudate activity under comparable behavioral conditions as in the present study (Ding and Gold 2010). All training, surgery, and experimental procedures were in accordance with the National Institutes of Health Guide for the Care and Use of Laboratory Animals and were approved by the University of Pennsylvania Institutional Animal Care and Use Committee.

Behavioral Task

The DOTS task is described in detail elsewhere (Fig. 1*A*; Roitman and Shadlen 2002). Briefly, the monkey fixated for a random time (between 0.3–3.0 s for monkey C and 0.4–2.5 s for monkey F, picked from a truncated exponential distribution to minimize anticipation of the end of this period), followed by dimming of the fixation point and onset of the motion stimulus. The stimulus was a random-dot kinematogram shown in a 5° aperture centered on the fixation point. Motion strength was specified as the percent of dots moving coherently in 1 of 2 directions (coherence, set to 0%, 3.2%, 6.4%, 12.8%, 25.6%, or 51.2%) at a fixed velocity of 6°/s. Motion direction and coherence were chosen randomly on each trial. The stimulus was immediately turned off when the monkey's gaze left the fixation window, which was a square with sides of length 4° for monkey C, 3.5° for monkey F. Despite these relatively large windows, both monkeys tended to maintain fixation within a much smaller window while performing the task: On average, the largest eye-position deviation from stimulus onset to 100 ms before saccade onset had a mean ± standard deviation (SD) of 0.49° ± 0.48° (Supplementary Fig. 1). Moreover, we found no consistent relationship between eye-position deviation along the axis of motion during motion viewing and the subsequent RT (mean r across sessions = –0.0025, t-test for zero mean, $P = 0.894$).

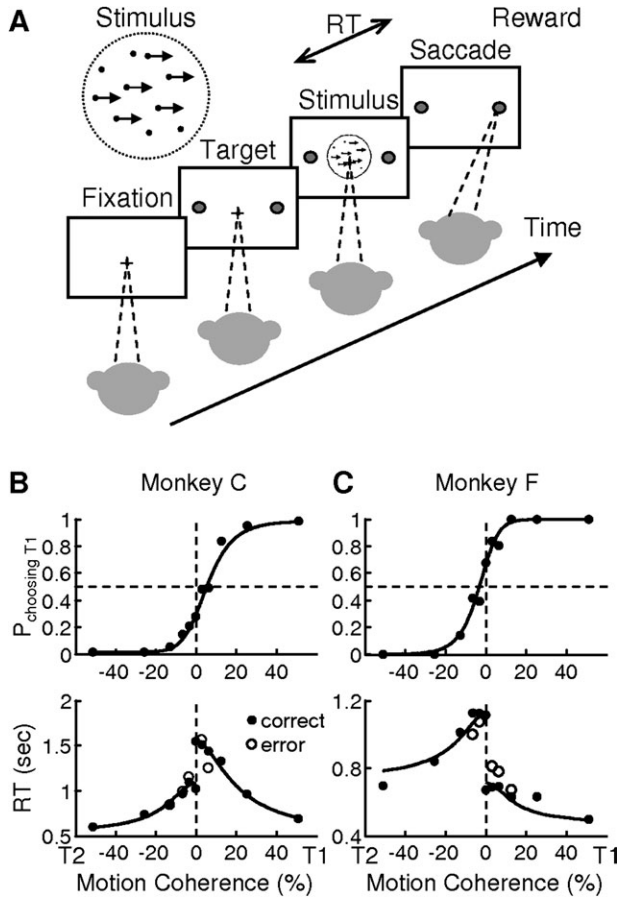

Figure 1. Behavioral task and performance. (*A*) The monkey decides the direction of random-dot motion and then responds immediately by making a saccade to 1 of 2 choice targets. Saccades to the target in the direction of coherent motion (assigned randomly for 0% coherence) are followed by a juice reward. (*B*,*C*) Example psychometric (top) and chronometric (bottom) functions from a single session for monkey C (*B*) and monkey F (*C*). Psychometric functions are plotted as the fraction of trials in which the monkey chose the T_1 target as a function of signed coherence, where positive coherence indicates motion toward T_1. Chronometric functions are plotted as the mean RT, measured as the time between motion-stimulus onset and saccade onset, for saccades toward each target, separated by correct (filled symbols) and error (open symbols) trials. Solid curves are simultaneous fits of both functions to a DDM with asymmetric bounds. Fitting parameters for the example shown for monkey C: $A = 44.40$, $B = 18.17$, $k = 0.29$, $T_{01} = 306.14$ ms, $T_{02} = 369.32$ ms; monkey F: $A = 12.59$, $B = 25.15$, $k = 0.58$, $T_{01} = 450.86$ ms, $T_{02} = 698.38$ ms.

The monkey was rewarded with a drop of juice for making a saccadic eye movement and then maintaining fixation for >400 ms on the target in the direction of coherent motion (or chosen at random on 0% coherence trials) at any time following the stimulus onset. Error feedback was given by extinguishing the error target while simultaneously turning on the correct target, followed by no reward and a time-out of 4–8 s. Before being trained on the DOTS task, Monkey C had been extensively trained for a different study. During the initial training on the DOTS task, this monkey developed the strategy of making repeated, fast choices to one target, while ignoring the motion stimulus. To discourage these fast guesses, a minimum of 1.5 s from stimulus onset to reward delivery was imposed. Monkey F was naïve before training for this study and thus no such minimal delay was set. Eye position was monitored using a video-based system (ASL) sampled at 240 Hz.

We used a standard MGS task to search for neurons and test for any relationship in FEF activity between the MGS and DOTS tasks. For the MGS task, the monkey fixated for 500–1000 ms, after which a peripheral cue was flashed for 100 ms at 1 of 8 possible locations. The monkey maintained fixation until the fixation point was turned off (GO signal) ~600 to 1000 ms after cue onset and was rewarded with a drop of juice 400 ms after a correct saccade to the memorized cue location.

Electrophysiology

Each monkey was implanted with a head holder and recording cylinder that provided access to the right FEF. Neural activity was recorded using glass-coated tungsten electrodes (Alpha-Omega) driven by a NaN microdrive (NAN Instruments, LTD) and sorted off-line (Plexon, Inc.). The FEF was identified as the anterior bank of the arcuate sulcus where saccades were evoked with microstimulation of <50 μA (70-ms trains of 300-Hz, 250-μs biphasic pulses) (Bruce et al. 1985). We searched for neurons while the monkeys performed the MGS task. We attempted to record from all cells that showed modulated activity on the DOTS task, identified by visual inspection of ~10 to 20 trials. We determined the direction axis for the DOTS task by finding the target location that elicited the largest responses, assessed qualitatively, on the MGS task, and placed one target (T_1) at that location, the other 180° opposite the fixation point (T_2).

Behavioral Data Analysis

We defined RT as the time from stimulus onset to saccade onset. Saccade onset was identified off-line with respect to velocity (>40°/s) and acceleration (>8000°/s^2). We used a drift-diffusion model (DDM) to fit choice (T_1 or T_2) and RT data simultaneously as functions of motion coherence (Palmer et al. 2005; Hanks et al. 2006). According to this model, momentary motion evidence is normally distributed, ~N(μ, 1), with a mean, μ, that scales with coherence: $\mu = k \times \mathrm{Coh}$, where k is a fit parameter that governs the coherence-dependent drift and Coh is the signed motion coherence (positive for toward T_1, negative for toward T_2). This momentary motion evidence is accumulated over time

until reaching 1 of 2 bounds, the identity of which governs choice (+A for T_1 or −B for T_2). Decision time is defined as the interval between stimulus onset and crossing of either decision bound. RT is the sum of decision time and nondecision time (T_{01} for a T_1 choice and T_{02} for a T_2 choice). The probability of choosing T_1 (i.e., the probability that the decision variable reaches bound +A first) is

$$P_{T_1} = \frac{e^{2\mu B} - 1}{e^{2\mu B} - e^{-2\mu A}} \quad (1a)$$

The average decision time is

$$\mathrm{DT}_{T_1} = \frac{A+B}{\mu}\coth\left(\mu\left(A+B\right)\right) - \frac{B}{\mu}\coth\left(\mu B\right) \quad (1b)$$

for T_1 choices and

$$\mathrm{DT}_{T_2} = \frac{A+B}{\mu}\coth\left(\mu\left(A+B\right)\right) - \frac{A}{\mu}\coth\left(\mu A\right) \quad (1c)$$

for T_2 choices. Best-fit parameters (A, B, k, T_{01}, and T_{02}) were obtained using maximum-likelihood methods. Threshold was estimated from the choice function as one-half the difference in coherence corresponding to 25% and 75% T_1 choices (Klein 2001). Bias was defined as the percent coherence corresponding to 50% T_1 choices.

Neural Data Analysis

For each neuron with stable recordings on ⩾10 correct trials per condition, we computed the average firing rates in 4 task epochs: 1) Stim, from 300 ms after stimulus onset to 100 ms before the median RT at 51.2% coherence (note that the duration of this epoch varied across sessions but was largely constant for all trials for a given neuron, except for trials with RTs shorter than the median RT at 51.2% coherence, for which the Stim epoch was terminated 100 ms before saccade onset); 2) Sac, from 100 ms before to 100 ms after saccade onset; 3) Post, from 100 to 500 ms after saccade onset; and 4) Rew, from reward onset to 500 ms afterward. For activity in each epoch, we examined the choice and coherence dependence using raw spike data from correct trials with nonzero coherence. If there was significant choice dependence (Wilcoxon rank-sum test for H_0: equal median spike rates in the given epoch from correct trials corresponding to the 2 choices = 0, $P < 0.05$), the choice associated with larger median activity was designated IN, the other OUT. For choice-independent activity, we arbitrarily assigned the choice associated with contralateral or up target as the IN choice, the other as the OUT choice, for display purposes only. An additional analysis tested for coherence dependence by computing a linear regression, with the coherence level and a constant term as the regressors, separately for IN and OUT choices. The significance of the coherence dependence was assessed using an F-test (H_0: slope = 0, $P < 0.05$).

We defined activity related to decision formation ("DDM-like") as choice-dependent activity in the Stim epoch that was modulated by coherence with different signs for the 2 choices. In other words, the choice-dependent activity could show coherence modulation for both choices, one with a positive coefficient and the other with a negative one or coherence modulation for one choice only. For each neuron with DDM-like activity, we tested for choice dependence after stimulus onset in 100-ms sliding windows at 10-ms steps and estimated the onset of choice-dependent activity, t_{choice}, as the beginning of the first 100-ms window with significant choice dependence (Wilcoxon rank-sum test, $P < 0.05$). Note that this measure only indicates that activity can be differentiated sometime between t_{choice} and t_{choice} +100 ms. We computed the unfiltered spike-density function between 200 ms before t_{choice} and the median saccade RT, excluding activity > 100 ms before saccade onset for each trial. We identified the time of highest/lowest activity, t_{peak}, for IN/OUT choice trials using a running average of the spike-density function (10-ms running window). We measured the rate of change during motion viewing as the slope of a linear fit to this running average between t_{choice} and t_{peak}, with coherence level and a constant term as the regressors.

We defined decision-trace activity as other activity that was modulated by coherence. We further subdivided this activity into 2 groups. Choice-dependent decision-trace activity was modulated by coherence with different signs for the 2 choices in the Sac, Post, and/or Rew epochs. The other decision-trace activity was modulated by coherence with the same sign for the 2 choices, regardless of additional (coherence-independent) modulation by choice.

We categorized the neuronal responses on the MGS task as visual, visuomovement, or movement, using similar criteria as a previous report (Cohen, Pouget, et al. 2009). Briefly, average firing rates were computed in 3 epochs: 100-0 ms before cue onset (baseline), 100–200 ms after cue onset (visual), and 100-0 ms before saccade onset (movement). Neurons with activity that was different from baseline (Wilcoxon rank-sum test, $P < 0.05$) in the visual or movement epoch alone were categorized as visual or movement neurons, respectively. Neurons that were active in both epochs were categorized as visuomovement neurons. We also identified neurons with persistent activity during a memory period (300-ms window before GO signal). Direction selectivity was assessed using activity associated with the same 2 directions as in the DOTS task (Wilcoxon rank-sum test, H_0: equal medians for the 2 directions, $P < 0.05$).

To distinguish putative inhibitory interneurons and excitatory pyramidal neurons, we measured the spike width as the time interval from the trough to the following peak of the average spike waveform for each neuron. Spike width in our sample was bimodally distributed (Fig. 8*A*), similarly to previous reports of cortical neurons (Constantinidis and Goldman-Rakic 2002; Tamura et al. 2004; Mitchell et al. 2007; Chen et al. 2008; Hussar and Pasternak 2009; Johnston et al. 2009; Song and McPeek 2010). Based on visual inspection of the spike-width histogram and consistent with previously used criteria for other cortical areas (Mitchell et al. 2007; Hussar and Pasternak 2009), we divided the neurons into 2 categories: narrow spike (spike width ⩽ 200 μs) and broad spike (spike width > 200 μs).

To quantitatively document the presence of a transient dip in activity after stimulus onset, for each neuron, we averaged neural activity across all conditions. From this average activity, we estimated the baseline activity in a 200-ms window before stimulus onset and located the trough during the 300-ms period after stimulus onset. If the activity level at the trough was 2 SD below the baseline activity, we noted the presence of a dip and the interval from the trough to stimulus onset was taken as the latency of the dip.

Results

We trained 2 monkeys on the DOTS task (Fig. 1*A*). As reported previously (Ding and Gold 2010), both monkeys performed nearly perfectly with average RTs of <1 s for motion coherences >~20%. As coherence decreased, accuracy tended to decrease and RT tended to increase (Fig. 1*B,C*). Both monkeys also exhibited slight choice biases, with monkey C exhibiting different tendencies depending on the axis of motion and monkey F always tending to choose rightward slightly more often and more quickly.

To quantify and better understand these trends in behavior, we fit both the psychometric and the chronometric data using a DDM (eq. 1; Fig. 1*B,C*; Palmer et al. 2005; Hanks et al. 2006; Ding and Gold 2010). The DDM is just one of several forms of "sequential-sampling model" (for a review, see Smith and Ratcliff 2004) and related neurally inspired models that have been used to describe behavior on this task (Mazurek et al. 2003; Ditterich 2006; Shadlen et al. 2006; Wong and Wang 2006; Grossberg and Pilly 2008). We used the DDM to show that our monkeys' behavior was compatible with the basic decision process described by these models, in which motion information is accumulated over time until reaching a fixed bound. Accordingly, our behavioral fits were similar to those reported elsewhere for either monkey or human subjects, although our RTs were longer (Mazurek et al. 2003; Palmer et al. 2005; Hanks et al. 2006). Our model also included

asymmetric decision bounds and nondecision time, which accounted for the choice and RT biases that we measured (for monkeys' overall performance and fitting parameter statistics, see Supplementary Fig. 2 and Supplementary Table 1). In general, these fits to the DDM facilitate our descriptions of FEF activity and comparisons to previously reported LIP and caudate activity from monkeys performing similar DOTS tasks and with comparable performance (Roitman and Shadlen 2002; Ding and Gold 2010).

We examined 95 FEF neurons whose activity was modulated during the DOTS task (n = 63 and 32 from monkeys C and F, respectively). We related the activity of these neurons to task performance (Parker and Newsome 1998; Gold and Shadlen 2007), by characterizing responses with respect to motion strength, choice, and the timing of task-related activation (summarized in Supplementary Fig. 3). For convenience, including the ability to make comparisons with previous studies, we consider in detail 2 general categories of response properties: first, those that, like in the DDM, appear to represent an accumulation of incoming motion information to a fixed bound and second, those continue to encode information about the motion stimulus even after decision formation. We also compare these response properties across neurons with different spike waveforms (presumably corresponding to interneurons and projecting neurons) and different visuomovement properties and finally compare the results to previous findings from caudate (Ding and Gold 2010) and LIP (Roitman and Shadlen 2002).

DDM-Like Activity: An Accumulation of Incoming Motion Evidence to a Fixed Bound

The first type of task-dependent activity was modulated by motion strength, RT, and choice during the Stim epoch. This activity was consistent with the computations described by the DDM, including a temporal accumulation of motion information to a fixed bound, that govern both choice and RT.

Two example neurons that had different spike waveforms but similar DDM-like responses during motion viewing are shown in Figure 2. The first neuron was activated more when the visual motion was up and to the left (solid lines, designated as IN trials) than when the motion was in the opposite direction (dashed lines, designated as OUT trials; Wilcoxon rank-sum test, H_0: equal median responses for the 2 directions, $P < 0.0001$; Fig. 2*A–C*). When collapsed across coherence levels, the activity began to differentiate between IN and OUT trials soon after stimulus onset (t_{choice} = 190 ms). On IN trials, the activity tended to build up more rapidly for higher coherences (slope of a linear regression of average firing rate vs. coherence = 0.25 spikes/s/%coh, H_0: slope = 0, F = 9.97, P = 0.0019; slope of a linear regression of the rate of rise in activity vs. coherence = 3.79 spikes/s^2/%coh, F = 66.07, P = 0.0039; Fig. 2*A*). In contrast, on OUT trials, activity was less extensively modulated but tended to be smaller for higher coherences (slope of a linear regression of average firing rate vs. coherence = –0.36 spikes/s/%coh, F = 24.61, $P < 0.0001$; the rate of fall in activity was not significantly modulated by coherence, P = 0.26; Fig. 2*A*). Aligned to saccade onset, the neuron's activity increased during motion viewing until reaching a peak value 25 ms before saccade onset of ~105 spikes/s (range:

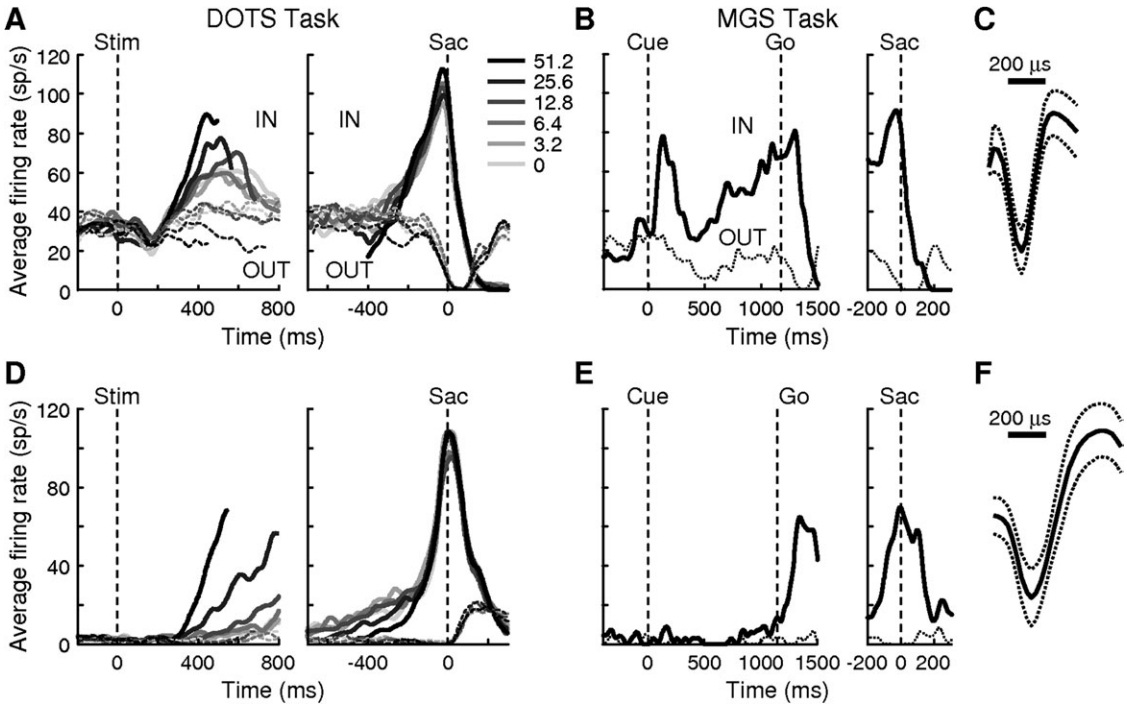

Figure 2. Example neurons with DDM-like activity. (*A–C*) An example neuron with narrow spikes (spike width = 175 µs). (*A*) Average activity of the neuron on the DOTS task, aligned to stimulus onset (left) and saccade onset (right). Activity following 100 ms before saccade onset was excluded in the left panel. Activity preceding 200 ms after stimulus onset was excluded in the right panel. Grayscales indicate coherence levels (see legend in *B*). Thick solid and thin dashed lines represent data from IN and OUT trials, respectively. Only correct trials and trials with zero coherence were included. Best-fitting DDM parameters from this session: A = 39.34, B = 20.86, k = 0.36, T_{01} = 341.40 ms, T_{02} = 400.29 ms. (*B*) Average activity of the neuron on the MGS task, aligned to cue onset (left) and saccade onset (right). Solid and dotted lines represent trials with the cue flashed at the IN and OUT target locations, respectively. (*C*) Spike waveform of the neuron (mean ± 2 SDs). (*D–F*) An example neuron with broad spikes (spike width = 375 µs). Same conventions as *A–C*. The behavioral data and DDM fits from this session are shown in Figure 1*B*.

95–112 spikes/s; Fig. 2*A*). On the MGS task, the neuron showed responses typical of an FEF visuomovement neuron, with a transient visual response, spatially selective delay-period activity in the absence of the cue, and a presaccadic burst (Fig. 2*B*). The spikes of this neuron were relatively narrow, with a trough-to-peak interval of 175 μs (Fig. 2*C*).

The second example neuron showed similar responses during motion viewing (Fig. 2*D–F*). This neuron also had a t_{choice} of 190 ms. The average spike rate in the Stim epoch was positively modulated by coherence on IN trials but not on OUT trials (IN slope = 0.25 spikes/s/%coh, F = 77.97, P < 0.0001; OUT slope = −0.0098 spikes/s/%coh, F = 2.03, P = 0.1559). The rate of change in activity as a function of viewing time during this epoch was also modulated by coherence for IN and OUT trials (slope = 1.68 and −0.37 spikes/s^2/%coh, F = 128.67 and 197.71, P = 0.0015 and 0.0008, respectively). Aligned to saccade onset, the neuron's activity increased during motion viewing until converging at ~60 spikes/s and reaching a peak value at 13 ms after saccade onset of 103 spikes/s (range: 95–108 spikes/s; Fig. 2*D*). On the MGS task, this neuron's responses were dominated by a saccadic burst typical of a movement neuron, with slight activation during the latter half of the delay period (Fig. 2*E*). Compared with the first example, this neuron had a lower baseline firing rate and broader spikes (Fig. 2*F*, trough-to-peak interval, 375 μs).

Across the population, we found DDM-like activity in 34 neurons (n = 26 and 8 for monkeys C and F, respectively; Fig. 3). Their activity became selective for choice after stimulus onset with a median t_{choice} of 235 ms (interquartile range: 170–280 ms). Consistent with how these neurons were selected, the average firing rate during a 100-ms window before the median RT for each coherence level was positively modulated by coherence on IN trials and negatively modulated on OUT trials (Fig. 3*C*). In addition, the activity developed gradually over the duration of the Stim epoch, in a coherence-dependent fashion (Fig. 3*E,F*). For IN trials, the rate of change in activity was positively modulated by coherence in 14 individual neurons, with a median slope of 1.88 spikes/s^2/%coh. For OUT trials, the rate of change in activity was negatively modulated by coherence in 4 neurons, with a median slope of −1.59 spikes/s^2/%coh. Across all 34 neurons, the median slopes were 1.37 and −0.17 spikes/s^2/%coh for IN and OUT trials, respectively, both significantly different from zero (Wilcoxon sign test, P = 0.0029 and 0.0243). These patterns of time, coherence, and choice dependence are similar to those observed in FEF of monkeys performing a fixed-duration version of the DOTS task (Kim and Shadlen 1999), both of which are consistent with a neural representation of accumulated evidence in the DDM but distinct from more transient direction-selective visual responses in FEF during passive viewing (Xiao et al. 2006).

The RT version of the DOTS task provides several advantages over the fixed-duration version, most notably allowing more direct examination of the time course and termination of the decision process. According to the DDM, stimulus strength plus noise governs the rate of evidence accumulation, which in turn governs RT when bound heights are fixed (Ratcliff and Smith 2004). The model thus predicts that the rate of rise of the decision variable should relate directly to RT and should relate to coherence only insofar as coherence affects RT. To test this prediction, for each neuron, we measured the average activity in a 200-ms window beginning at t_{choice} and performed

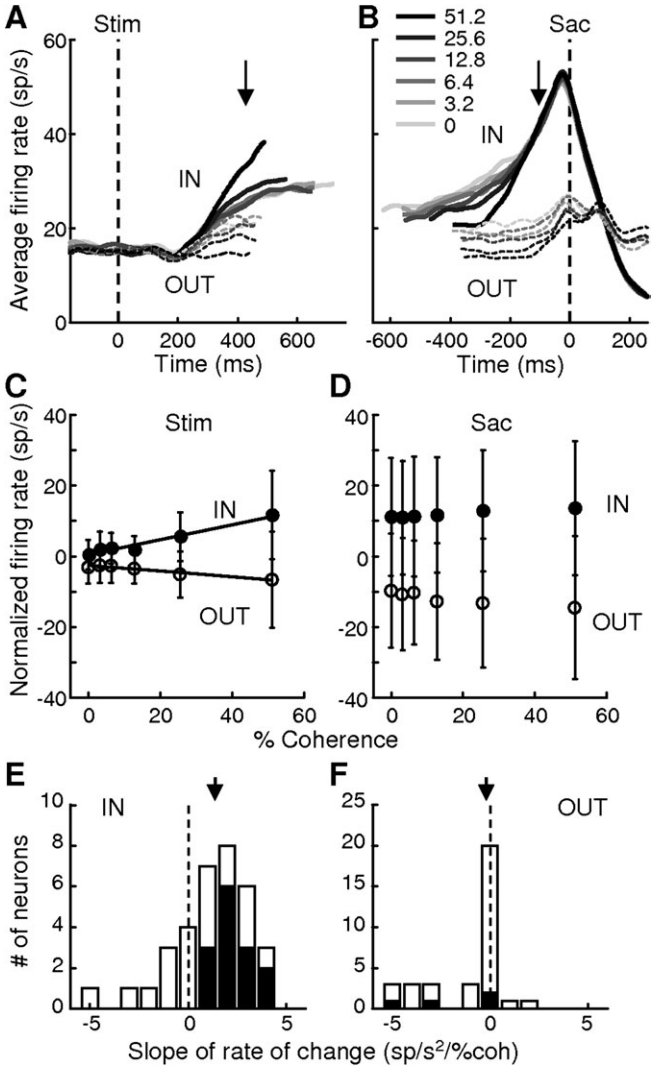

Figure 3. Population DDM-like activity. (*A*) Population average of activity aligned on stimulus onset for correct trials (n = 34). Data for each choice (solid lines, IN trials; dashed lines, OUT trials) and coherence level (grayscales, see legend in *B*) were truncated at the median value of the mean RT measured under those conditions for all cells. Activity following 100 ms before saccade onset was excluded. (*B*) Population average of activity aligned on saccade onset, plotted as in *A*. Activity preceding 200 ms after stimulus onset was excluded. (*C,D*) Population average (mean ± standard error of the mean) of normalized firing rate as a function of coherence in 100-ms windows before the median RT (arrow in *A*, which indicates only an approximate time because of session-by-session variability in mean RT) and before saccade onset (arrow in *B*), respectively. For each neuron, the firing rate in an epoch was normalized by the average rate across all trial conditions in the same epoch. Filled circles: IN trials; open circles: OUT trials. Lines in *C* are linear fits with slopes that were significantly different from zero (slopes = 0.21 and −0.08 spikes/s/%coh, F = 58.87 and 7.84, P < 0.0001 and P = 0.0056, for IN and OUT trials, respectively). Slopes were not significantly different from zero for data points in *D* (P = 0.42 and 0.18 for IN and OUT trials, respectively). (*E,F*) Histograms of the slope of the rate of rise in activity during motion viewing for IN (*E*) and OUT (*F*) trials. Arrows indicate median values. Solid bars: F-test, H_0: slope = 0, P < 0.05.

separate linear regressions with RT for each coherence level and regressions with coherence for fixed ranges of RT. From regressions with RT, we observed significant negative (positive) slopes for neural activity on IN (OUT) trials at most coherence levels (Table 1), suggesting a link between neural activity and decision time that was independent of motion strength. From regressions with coherence, there was no

significant slope in any RT ranges for either IN and OUT trials, with a single exception for IN trials with long RTs (Table 2), suggesting that the observed coherence modulation was secondary to the link between neural activity and RT. The difference in the regression coefficients with RT for each coherence level versus with coherence for fixed ranges of RT is also graphically illustrated in Supplementary Figure 4.

FEF activity is also consistent with the termination process described by the DDM, in which evidence is accumulated until reaching a fixed bound (Ratcliff and Rouder 1998; Roitman and Shadlen 2002). In particular, several analyses indicate that FEF DDM-like activity rose to a common value just before saccade onset. First, when aligned on saccade onset, population average activity rose in a coherence-dependent manner but then reached a common, coherence-independent level just before saccade onset: the coherence dependence that was present earlier in the Stim epoch (Fig. 3*A*,*C*) was absent just before saccade onset (Fig. 3*B*,*D*). Second, if a fixed decision bound is present, then activity at bound crossing should be independent of coherence. Moreover, activity before bound crossing should be positively modulated by coherence when aligned to stimulus onset but negatively modulated by coherence when aligned to saccade onset because activity rose faster on high-coherence trials. These patterns of coherence modulation were evident in the population average activity (Fig. 4*A*), as well as in a substantial proportion of individual neurons (Fig. 4*C*). Thirteen neurons showed significant negative coherence modulation 200–300 ms before saccade onset and no coherence modulation 100 ms before saccade onset. A reverse

Table 1
Summary statistics of RT regression for different coherence levels

%Coherence	Slope (IN)	*P* value	Slope (OUT)	*P* value
3.2	−12.1363	**0.0021**	−0.5926	0.2153
	−4.5063		0.3911	
	0		10.8049	
6.4	−15.5911	**0.0013**	−0.7771	0.0801
	−7.9363		1.4625	
	−0.3202		12.8620	
12.8	−14.4153	**0.0008**	0	**0.0046**
	−9.287		**1.9448**	
	−0.8541		7.2945	
25.6	−29.8433	**0.0008**	−0.7619	0.0501
	−9.3275		2.8983	
	−1.4403		9.4144	
51.2	−24.8827	0.3915	0	**0.0003**
	−5.6266		**4.5149**	
	13.2888		32.0167	

Note: Analyses were performed on the average spike rate of DDM-like activity in a 200-ms window after t_{choice} as a function of RT at different coherence levels. Slope data are in units of spikes/s^2 and presented as 25/50/75 percentiles across neurons. *P* values are from a 2-sided sign test (H_0: slope = 0). Bold items: $P < 0.05$.

Table 2
Summary statistics of regression with coherence for different RT groups

RT groups (ms)	Slope (IN)	*P* value	Slope (OUT)	*P* value
<500	−0.0847	0.3833	−0.2243	1
	0.0349		0	
	0.1594		0.0148	
500–700	−0.0526	0.2295	−0.1433	0.2153
	0.0422		−0.0147	
	0.1438		0.0220	
700–900	−0.0242	0.1102	−0.0330	0.845
	0.0723		0	
	0.1264		0.0990	
900–1100	−0.3035	0.7201	−0.1657	0.4244
	−0.0159		−0.0123	
	0.0821		0.0791	
1100–1300	−0.3932	0.8145	−0.0784	0.4049
	−0.0543		−0.0149	
	0.1402		0.2537	
1300–1500	−0.6209	**0.0039**	−0.2166	0.8238
	−0.1660		−0.0257	
	−0.0903		0.1158	

Note: Analyses were performed on the average spike rate of DDM-like activity in a 200-ms window after t_{choice} as a function of coherence for trials with different RTs. Slope data are in the unit of spikes/s/%coh and presented as 25/50/75 percentiles across neurons. *P* values are from a 2-sided sign test (H_0: slope = 0). Bold items: $P < 0.05$.

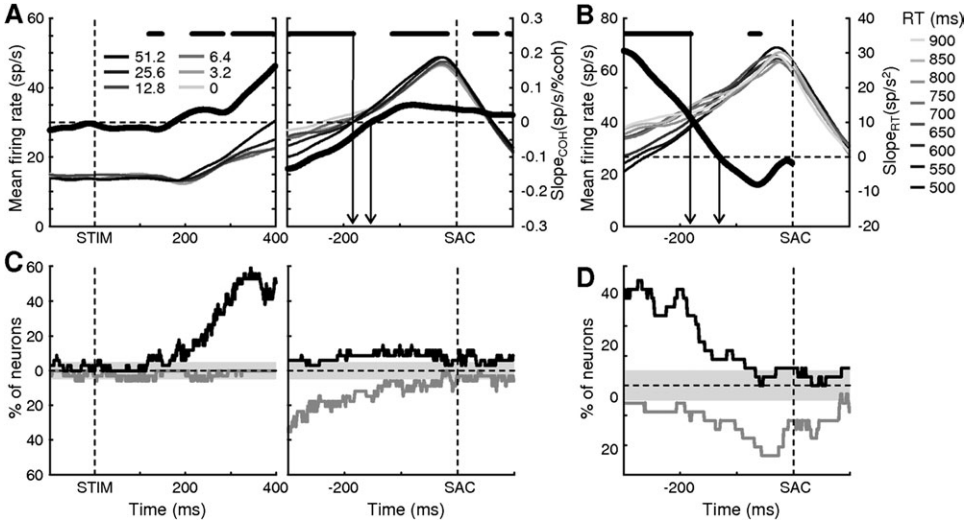

Figure 4. DDM-like activity increased toward a decision bound. (*A*) Regression slope values (thick black lines, right axes) of population average activity (thin lines, left axes) aligned on stimulus (left panel) and saccade (right panel) onset, with motion coherence as the regressor. Grayscales indicate coherence levels. Black bars on top indicate time bins with slope value significantly different from zero (*t*-test, $P < 0.05$). Arrows indicate estimates of when activity converged to a common level (left: the last window with a significant negative slope; right: the time window when the slope value crosses zero). (*B*) Regression slope values of population average activity aligned on saccade onset, with RT as the regressor. Grayscales indicate the starting value of each RT bin (bin size = 50 ms). Same conventions as *A*. (*C*) Percentage of neurons showing a significant slope from the regression with coherence. Black: positive slopes; gray: negative slopes; light gray areas indicate 5% chance level. (*D*) Percentage of neurons showing a significant slope from the regression with RT. Same conventions as *C*.

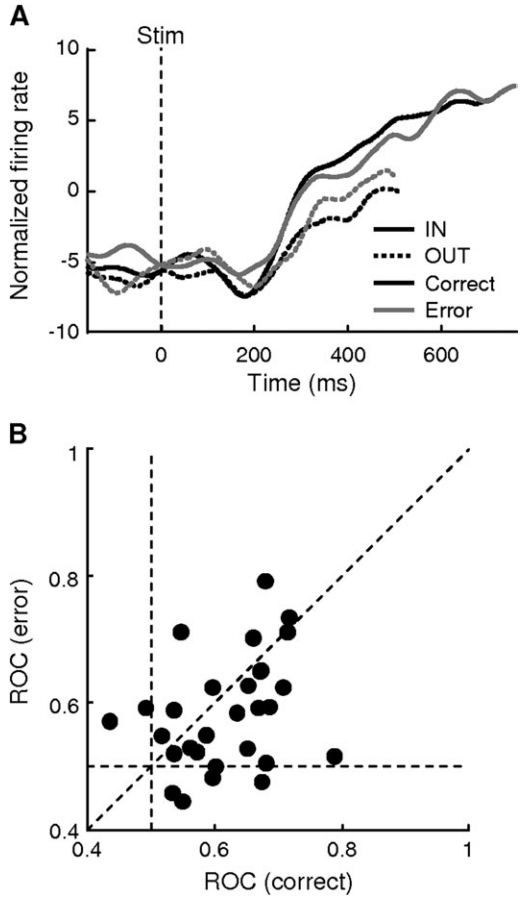

Figure 5. Comparison of DDM-like activity for error and correct trials with weak motion strength. (*A*) Population average of activity from neurons with DDM-like activity for correct (black) and error (gray) trials at 3.2% coherence. Solid lines, IN choice; dotted lines, OUT choice. Data were truncated at the minimum value of the median RT measured under those conditions for all cells and standardized by subtracting the average firing rate 200–600 ms after stimulus onset for all trials for a given cell. (*B*) Scatter plot of the ROC indices computed using the average firing rate within a 300-ms window beginning at t_{choice}, excluding activity within 100 ms of saccade onset, for 3.2% coherence trials. $n = 32$ (two sessions did not have sufficient error trials for this analysis).

pattern is predicted for activity grouped by RTs and was observed in FEF, as well (Fig. 4*B*,*D*).

To estimate the timing of convergence, we tracked the coherence modulation and RT modulation of average activity for 400 ms before saccade onset, in 1-ms steps. Using activity grouped by coherence, we defined the last time point with a significant negative slope ($P < 0.05$) and the time point when slope crossed zero as the upper and lower bounds of the convergence time, respectively (arrows in Fig. 4*A*). Using this definition, the population activity converged 152–183 ms before saccade onset. Using activity grouped by RT, we defined the last time point with a significant positive slope ($P < 0.05$) and the time point when slope crossed zero as the upper and lower bound of the convergence time, respectively (arrows in Fig. 4*B*). Using this definition, the population activity converged 130–181 ms before saccade onset. Note that after this convergence time, the population average activity showed positive coherence- and small negative RT modulation around saccade onset due to convergence patterns of different cell types (see below).

With the assumption that the convergence time of FEF activity reflects the time of decision commitment, the remaining delay to saccade onset may be thought of as the motor component of nondecision time in the DDM. With the assumption that choice-selective activity first emerges at the beginning of evidence accumulation, t_{choice} may be thought of as the sensory component of nondecision time in the DDM. In our sample, the nondecision time from the DDM model fits of the monkey's behavior (median value of 396 ms for saccades to the preferred targets for the recorded neurons) was within the range of the sum of t_{choice} (median: 235 ms; interquartile range: 170–280 ms) and the convergence-to-saccade delay (~130 to 183 ms). When separated by motion axis, the difference between the nondecision time and t_{choice} was 140–229 ms, roughly consistent with the estimate of the convergence-to-saccade delay. These results suggest a close link between FEF DDM-like activity and the monkey's behavioral responses.

This link can also be appreciated by comparing correct and error trials (Fig. 5). Activity was different between trials with IN and OUT choices, even when the motion direction was the same (Fig. 5*A*). When the motion direction was toward the IN target, activity was higher if monkey subsequently chose the IN target (correct choice, black solid line) than if monkey chose the OUT target (error choice, gray dashed line). When the motion direction was toward the OUT target, activity was also higher if monkey subsequently chose the IN target (error choice, gray solid line) than if monkey chose the OUT target (correct choice, black dashed line). Thus, DDM-like activity was more correlated with the monkeys' perceptual reports than with the sensory stimulus, consistent with previous results using other tasks (Thompson, Bichot, et al. 2005; Trageser et al. 2008). Because the evidence supporting an error choice (e.g., an IN choice when the noisy motion stimulus was toward the OUT target) is weaker than a correct choice (e.g., an IN choice when the noisy motion stimulus was toward the IN target), the DDM further predicts that the rate of accumulation is lower in error than correct trials. Consistent with this prediction, the difference in activity between trials in which the monkey chose IN versus OUT targets, measured using an ROC-based index, was significantly smaller for error trials than for correct trials (Fig. 5*B*; Wilcoxon paired signed rank test, H_0: equal median, $P = 0.0126$).

Decision-Trace Activity: Coherence Dependence after Decision Formation

The second type of task-dependent activity was modulated by motion strength, with (blue circles in Supplementary Fig. 3*B*) or without (red circles in Supplementary Fig. 3*B*) additional modulation by choice. This activity tended to maintain information about stimulus strength even after the decision was made, possibly contributing to an ongoing evaluation of the decision process.

Similar to the DDM-like activity found during the Stim epoch, choice-dependent decision-trace activity differentiated between choices and was modulated by coherence with different signs for the 2 choices, with 39, 41, and 51 neurons showing this type of activity in the Sac, Post, and Rew epochs, respectively ($n = 56$ and 22 total neurons for monkeys C and F, respectively; Fig. 6). Negative slopes were more frequently observed for OUT trials in the Sac epoch and for IN trials in the Rew epoch. Positive slopes were more frequently observed for IN trials in the Post epoch and for OUT trials in the Rew epoch.

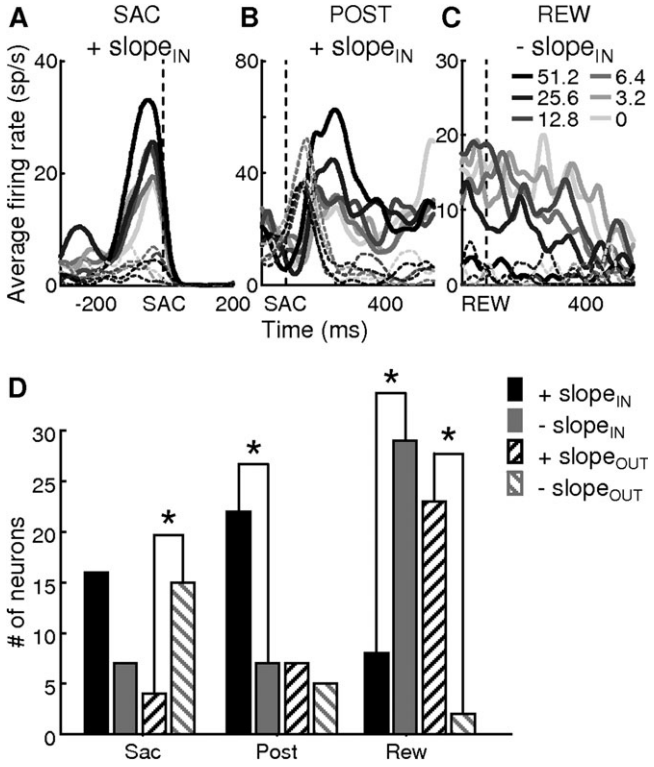

Figure 6. Choice-dependent decision-trace activity. (*A–C*) Three example neurons showing choice-dependent decision-trace activity. Same conventions as Figure 3*A*. (*A*,*B*). Activity in the Sac and Post epochs, respectively, increasing as a function of coherence for IN trials (+slope$_{IN}$). (*C*). Activity in the Rew epoch decreasing as a function of coherence for IN trials (−slope$_{IN}$). (*D*) Summary of choice-dependent decision-trace activity, grouped by the epoch and the sign of the slope from a linear regression with coherence for IN and OUT trials separately. "+slope" indicates increasing activity as a function of increasing coherence. "−slope" indicates decreasing activity as a function of increasing coherence. *: binomial test, H_0: same frequency of positive and negative slopes, $P < 0.05$, corrected for 6 comparisons.

Thus, after a decision is reached, a subset of FEF neurons could maintain information about the choice and the strength of motion evidence leading to that choice, providing various signals to facilitate evaluation of the decision process.

Another, less frequently observed, form of decision-trace activity was modulated by motion strength with the same sign for the 2 choices. Two example neurons are shown in Figure 7. The first neuron showed opposite coherence modulation in the Stim and Rew epochs. In the Stim epoch, activity was higher on low-coherence trials, for both rightward and leftward choices (Fig. 7*A*, left panels). In the Rew epoch, activity was higher on high-coherence trials, regardless of the actual choice the monkey just made (Fig. 7*A*, right panels). The second example neuron had higher activity on high-coherence trials for both choices in the Rew epoch only (Fig. 7*B*). In the population, activity that was modulated by motion strength with the same sign for the 2 choices occurred primarily in the Rew epoch ($n = 16$), with 10 and 6 neurons showing positive and negative slopes from a linear regression with motion coherence, respectively. Because motion coherence largely determines trial difficulty, the activity was also correlated with reward probability estimated for each individual session (Fig. 7*C*,*D*). Of 20 sets of trials (2 choices per neuron) with neural activity that was positively modulated by coherence, 15 also showed a positive correlation between neural activity and reward probability. Of 12 sets of trials with neural activity that was negatively modulated by coherence, 9 showed a negative correlation between neural activity and reward probability.

Comparison of Neurons with Narrow versus Broad Spike Waveforms

So far we have shown that 2 general types of decision-related activity are present in the FEF population. Next, we examined how these types of activity are distributed across different cell types in FEF. In particular, we focused on pyramidal neurons, presumably excitatory neurons that project to other subcortical and cortical areas, and interneurons, presumably inhibitory neurons that help shape local response properties

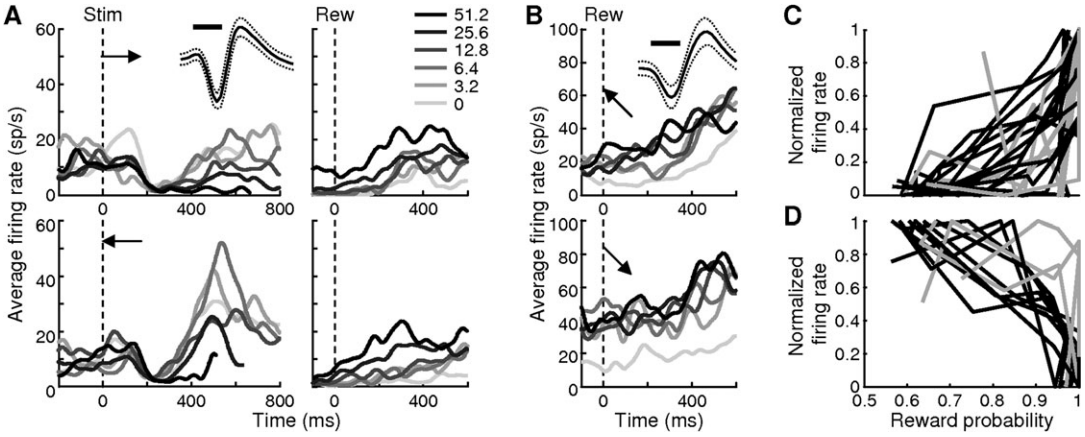

Figure 7. Decision-trace activity with same-sign coherence modulation for both choices. (*A*) An example neuron with narrow spikes (spike width = 175 μs). Average activity aligned to the onset of stimulus (left) and reward (right). Activity following 100 ms before saccade onset was excluded in the left panel. Grayscales indicate coherence levels. Top and bottom rows represent data from trials with motion direction indicated by the arrows in the left panel. Only correct trials and trials with zero coherence were included. The inset shows the spike waveform of the neuron (mean ± 2 SDs). (*B*) An example neuron with broad spikes (spike width = 250 μs). Same conventions as *A*, except that only activity around reward onset was shown. (*C*,*D*) Mean normalized Rew-epoch activity as a function of reward probability estimated from the monkey's behavior in the same session, for neurons with positive (*C*) and negative (*D*) slopes from a linear regression of neural activity with motion coherence ($n = 10$ and 6, respectively). Only trials with nonzero coherence were included. Lines connect data points from the same choice trials of a given cell (black lines: $P < 0.05$, *F*-test, H_0: slope from linear regression with reward probability = 0; gray lines: $P \geq 0.05$). Note that each cell is represented by 2 lines, corresponding to the 2 choices.

in several computational models (Usher and McClelland 2001; Wang 2002; Beck et al. 2008). Previous studies of FEF and other cortical areas have shown that putative pyramidal neurons tended to have broader spikes and lower baseline firing rate than putative interneurons (Rao et al. 1999; Constantinidis and Goldman-Rakic 2002; Tamura et al. 2004; Shin and Sommer 2006; Mitchell et al. 2007; Hussar and Pasternak 2009; Johnston et al. 2009; Song and McPeek 2010). Consistent with these studies, we observed a bimodal distribution of spike width in our sample (Hartigan's Dip test, $P < 0.0001$; Fig. 8*A*). With a cutoff width of 200 μs, neurons with narrow spikes had significantly higher baseline firing rate than neurons with broad spikes (median spike rate = 13.21 and 6.25 sp/s, $n = 43$ and 52, respectively, Wilcoxon rank-sum test, $P = 0.0004$).

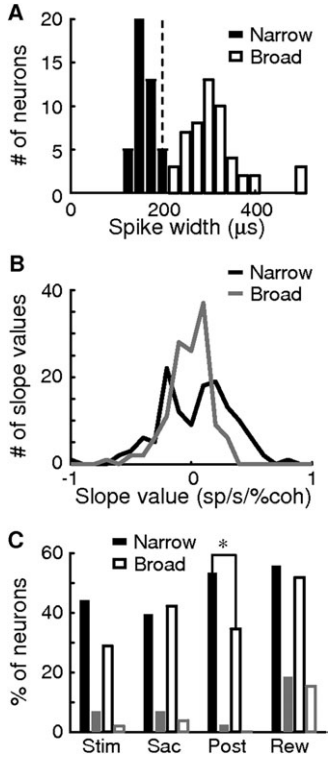

Figure 8. Response profiles of 2 classes of neurons based on spike width. (*A*) Histogram of spike width for all neurons. Dashed line indicates the boundary for the 2 classes (200 μs). (*B*) Histograms of slope values from a linear regression of neural activity with motion coherence for neurons with narrow (solid) and broad (open) spikes, including values from all epochs of all recorded neurons. (*C*) Percentage of neurons with narrow (solid bars) and broad (open bars) spikes showing DDM-like (black in Stim epoch), choice-dependent decision-trace (black in Sac, Post, and Rew epochs), and the other decision-trace (gray) activity in the 4 epochs. *: binomial test, H_0: same percentage for narrow- and broad-spike classes, $P < 0.05$, corrected for 8 comparisons.

Both classes of neurons showed qualitatively similar patterns of activity on the DOTS task, including similar distributions of DDM-like and decision-trace activity (Supplementary Fig. 5*A,B*). However, there were some quantitative differences. For example, the distribution of slope amplitudes from a linear regression of spike rate versus coherence was wider for neurons with narrow than with broad spikes (Wilcoxon rank-sum test of the absolute values of regression slopes, $P < 0.0001$, Fig. 8*B*; and note more red and dark blue bars in Supplementary Fig. 5*A* than in Supplementary Fig. 5*B*), possibly because of their higher baseline and peak firing rates (Fig. 9). Both classes of neurons were more likely to exhibit DDM-like and choice-dependent decision-trace activity than decision-trace activity with same-sign coherence modulation, with higher percentages choice-dependent decision-trace activity in the Post epoch for neurons with narrow versus broad spikes (Fig. 8*C*).

In addition to these differences in distributions across epochs, DDM-like activity differed between neurons with narrow and broad spikes in 4 other aspects. First, a transient dip in activity occurred at ~200 ms after motion-stimulus onset in a subset of neurons (see the example neuron in Fig. 2*A* and population average in Fig. 9*A,B*), similar to previously reported dip in LIP activity on the DOTS task and a preexcitation pause in FEF activity on visual-search and countermanding tasks (Sato and Schall 2001; Roitman and Shadlen 2002), albeit with longer latency. A larger proportion of neurons with broad spikes than with narrow spikes showed such a dip in activity (13 of 15 vs. 10 of 19 neurons with broad and narrow spikes, respectively; binomial test, $P = 0.001$), with similar latency and amplitude (Wilcoxon rank-sum test, $P = 0.1138$ for both measures).

Second, the difference in choice-dependent activity between the Stim and Sac epochs tended to be larger for neurons with narrow spikes (median values: 29.6 and 5.45 sp/s for narrow- and broad-spike neurons, respectively; Wilcoxon rank-sum test, $P = 0.0343$; Fig. 9*C*). As shown in Figure 9*A,B*, the population average activity was higher initially for neurons with narrow spikes, consistent with their higher baseline firing; attained

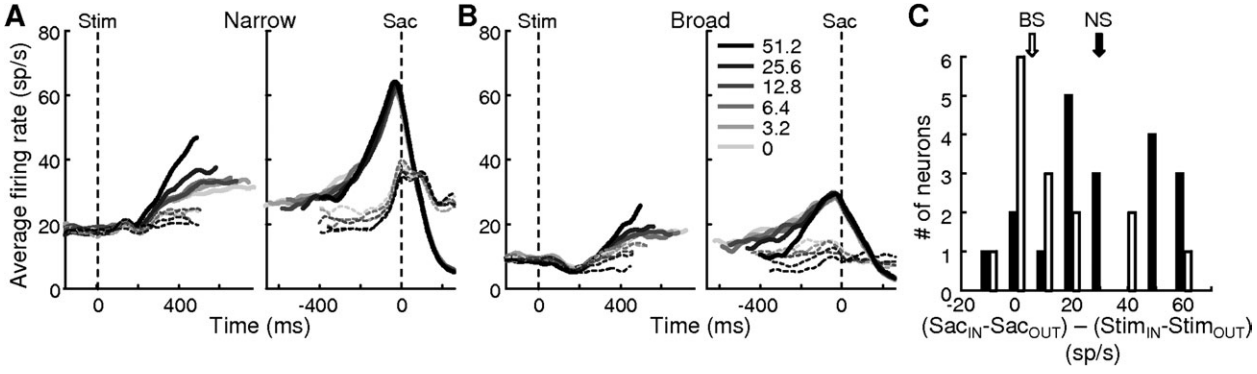

Figure 9. DDM-like activity has a larger saccade component in neurons with narrow versus broad spikes. (*A,B*) Population average activity of neurons with narrow (*A*) and broad (*B*) spikes with DDM-like activity ($n = 19$ and 15, respectively). Same conventions as Figure 3*A,B*. (*C*) Histogram of the difference in activity between Sac and Stim epochs for neurons with narrow (solid bars) or broad (open bars) spikes. Activity for each epoch is defined as the difference in activity between IN and OUT trials. Arrows indicate median values.

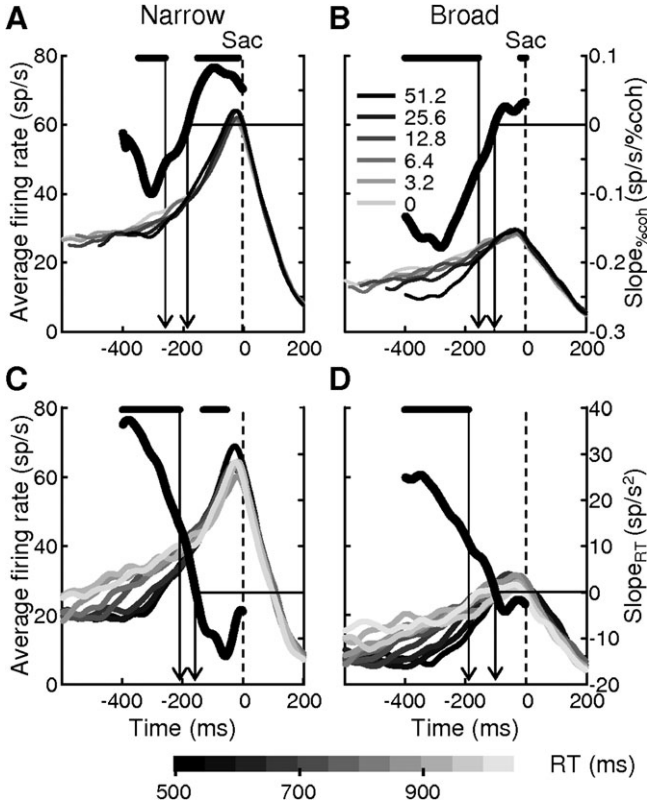

Figure 10. Timing of activity convergence before saccade onset for neurons with narrow (left) or broad (right) spike waveforms. (*A*,*B*) Estimates of the convergence time using activity grouped by motion coherence for neurons with DDM-like activity (n = 19 and 15, respectively). Thin lines (left axis) represent the population average activity (same as in Fig. 9*A*,*B*, right panels). Thick black lines (right axis) represent the slope values from a linear regression with motion coherence in a 400-ms window before saccade onset. Black bars on top indicate time bins with slope values significantly different from zero (F-test, $P < 0.05$). Arrows indicate estimates of when activity converged to a common level (left: the last window with a significant negative slope; right: the time window when the slope value crosses zero). (*C*,*D*) Estimates of the convergence time using activity grouped by RT. Same conventions as *A* and *B*, except that the grayscales indicate the starting values of RT groups (bin size, 50 ms; e.g., group 500 includes RTs in the range of 500–550 ms), and the slope values came from the regression of neural activity with RT.

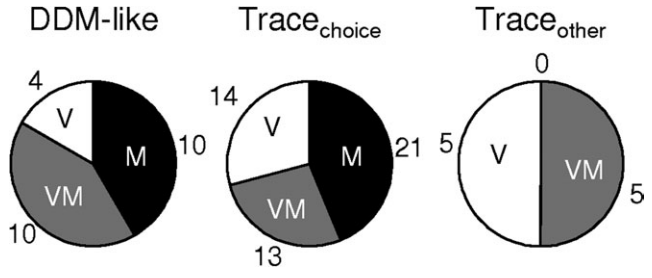

Figure 11. Summary of response profiles on the DOTS task for conventional neuron categories defined using activity on the MGS task. V: visual; VM: visuomovement; M: movement. For definitions, see Materials and Methods. Numbers indicate the numbers of neurons in each category. Fifty-nine neurons were included in this analysis. A single neuron may show multiple types of activity.

similar deviation from baseline ~400 ms after stimulus onset; and rose sharply before saccade onset in neurons with narrow spikes and more gradually in neurons with broad spikes.

The third and fourth differences between the 2 classes of neurons were in the timing and pattern of convergence to the common value, respectively. The timing of convergence was closer to saccade onset in neurons with broad spikes (Fig. 10; also compare the 2 example neurons in Fig. 2). By the same definitions as described above for population activity grouped by coherence, the activity of neurons with narrow spikes converged 185–259 ms before saccade onset, whereas the activity of neurons with broad spikes converged 104–157 ms before saccade onset. Based on population activity grouped by RT, the activity of neurons with narrow spikes converged 158–210 ms before saccade onset, whereas the activity of neurons with broad spikes converged 100–189 ms before saccade onset. After this convergence point, activity in neurons with narrow spikes showed positive coherence modulation and negative RT modulation, whereas activity in neurons with broad spikes showed little dependence on coherence or RT. Together, these results suggest that neurons with broad spikes are more closely linked to decision commitment.

Comparison of Response Patterns across Tasks

Previous studies of evidence-accumulation activity in LIP and FEF focused on neurons with persistent activity in the absence of visual stimulus (Shadlen and Newsome 1996, 2001; Kim and Shadlen 1999; Roitman and Shadlen 2002), leading to the impression that the latter is a prerequisite of the former. FEF neurons in conventional categories (e.g., visual, movement, and visuomovement) have been shown to serve different purposes for target discrimination during visual search (Schall, Hanes, et al. 1995; Thompson et al. 1996 Purcell et al. 2010) and for saccade preparation during saccade-countermanding tasks (Ray et al. 2009). We examined how these response categories relate to neural computations for motion discrimination.

To compare responses on the DOTS and MGS task, we focused on 59 neurons from which sufficient data were obtained on the MGS task to allow categorization into 1 of the 3 categories (n = 17, 19, and 23 for visual, visuomovement, and movement neurons, respectively). As shown in Figure 11, DDM-like activity was observed primarily in visuomovement and movement neurons, choice-dependent decision-trace activity was observed in all cell types, and other decision-trace activity (for the reward epoch only) was observed in visual and visuomovement, but not movement, neurons. Neurons with direction-selective persistent activity in the memory period on the MGS task were more likely to exhibit DDM-like activity (17/31 vs. 7/28, chi-square test, P = 0.0198). The 7 neurons that did not show such persistent activity included 2, 1 and 4 visual, visuomovement, and movement neurons, respectively. These results suggest that in FEF, movement-related activity on the MGS task is more closely associated with DDM-like activity on the DOTS task. However, all 3 types of neurons tended to have stronger choice selectivity on correct than on error trials, suggesting that all 3 encode information more closely linked to the decision than to the motion stimulus (Supplementary Fig. 6). We also confirmed a previously reported relationship between a neuron's response on MGS task and its spike width (Cohen, Pouget, et al. 2009): Visuomovement neurons have significantly shorter spikes than visual or movement neurons (Kruskal–Wallis test, χ^2, 15.04; multiple comparison procedure, $P < 0.05$).

Comparison of FEF and Caudate

The FEF and caudate data sets from the same monkeys on the same task allowed us to make direct comparison of task-related neural activity in the 2 brain regions (Ding and Gold 2010). The slope values from a linear regression of activity versus motion

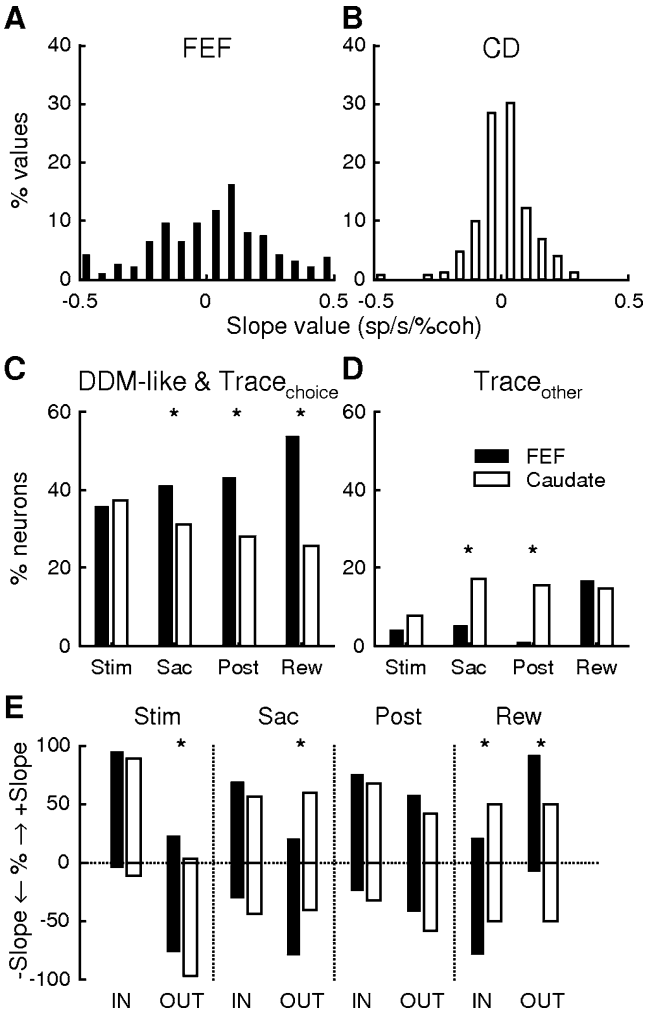

Figure 12. Comparison between FEF and caudate neurons on the DOTS task. (*A*,*B*) Histograms of the slope values from a linear regression of neural activity versus motion coherence during motion viewing for FEF (*A*) and caudate (*B*) neurons with choice-dependent coherence modulation, including values from all epochs of all recorded neurons. (*C*,*D*) Percentage of neurons showing activity with different (*C*) or similar (*D*) coherence modulation for the 2 choices for FEF (solid) and caudate (open) neurons in the 4 epochs. (*E*) Percentage of FEF (solid) and caudate (open) neurons with activity that increased ("+Slope") or decreased ("−Slope") as a function of motion coherence for choices IN or OUT relative to the neuron's RF in the 4 epochs. Only cells from *C* are included. Asterisks indicate $P < 0.05$, binomial test with correction for multiple comparisons.

coherence tended to distribute over a larger range in FEF neurons than in caudate neurons (Fig. 12*A*,*B*, Wilcoxon rank-sum test on absolute slope values, $P < 0.0001$), possibly because of their higher peak firing rates. Both regions contain neurons with choice- and coherence-dependent activity in all 4 epochs, with overall higher prevalence in FEF except for the Stim epoch (Fig. 12*C*). In contrast, decision-trace activity without strong choice dependence was observed significantly less frequently in FEF than in caudate in the Sac and Post epochs (Fig. 12*D*). Activity before stimulus onset that was predictive of choice, which was observed in ~10% of caudate neurons with choice-dependent activity in the Stim epoch, was rarely encountered in FEF (1/79, data not shown).

Although FEF and caudate had a similar prevalence of evidence-accumulation activity during the Stim epoch, their activity patterns were strikingly different in several aspects. First, this activity in FEF rose to a common level of activity just before saccade onset, a convergence pattern that was absent in caudate. Second, the onset of choice dependence in DDM-like activity after stimulus onset (t_{choice}) was significantly later in FEF than that of evidence-accumulation activity in caudate (FEF: median 235 ms, IQR: 170–280 ms; caudate: median 170 ms, IQR: 142.5–225 ms; Wilcoxon rank-sum test, $P = 0.0143$). Third, there were a slightly larger percentage of FEF neurons showing positive slopes of the activity-versus-coherence linear regressions for data from OUT trials (Fig. 12*E*, Stim epoch).

There were also significant differences in the details of decision-trace activity. For choice-dependent decision-trace activity, caudate neurons tended to show similar prevalence of positive and negative modulation by coherence (Fig. 12*E*), whereas FEF neurons tended to show a preference in OUT choice trials in the Sac epoch (negative dominant), IN choice trials in the Rew epoch (negative dominant), and OUT choice trials in the Rew epoch (positive dominant). For choice-independent trace activity in the Rew epoch, FEF neurons were more often positively modulated by coherence, whereas the majority of caudate activity was negatively modulated by coherence ($P = 0.0005$, binomial test).

Discussion

We have shown that, in monkeys performing an RT version of the DOTS task, activity of many individual FEF neurons depended on the monkey's saccadic choice and/or the strength of the motion stimulus used to generate that choice. We classified activity during motion viewing that was modulated by choice, motion strength, and RT as DDM-like because of its relationship to the dynamics of decision formation in those models. We classified other activity that depended on motion strength, either with or without an additional choice dependence, after motion viewing as a "decision trace" because it encoded decision-related information even after the decision was formed. Both kinds of activity were distributed across neuronal types classified by waveform shape or visuomotor properties, suggesting that decision-related processing in FEF is not limited to particular subsets of neurons. Below we discuss in detail these 2 types of activity and their distribution across subsets of FEF neurons and other brain regions (LIP and caudate) tested under similar conditions.

DDM-Like Activity

The motivation for interpreting our data in terms of the DDM framework—a form of sequential analysis that, under certain assumptions, is consistent with statistically optimal procedures for reaching this kind of noisy 2-choice decision (Wald and Wolfowitz 1948; Good 1979, 1983; Gold and Shadlen 2007)—was its past success at describing behavior and neural activity associated with the DOTS task. For versions of the task in which the experimenter provides variable-duration stimuli to monkeys, their performance improves as a function of viewing time in a manner consistent with a temporal integration of incoming motion evidence, as predicted by the model (Gold and Shadlen 2002, 2003). For RT (and possibly variable duration) versions of the task, this accumulation process is thought to terminate by reaching a predefined bound that determines both choice and reaction time (Roitman and Shadlen 2002; Mazurek et al. 2003; Palmer et al. 2005; Kiani et al. 2008). Neural correlates of the accumulation process have been identified in FEF, LIP, and SC using a fixed-duration version of

the DOTS task and in LIP and caudate using an RT DOTS task (Shadlen and Newsome 1996; Horwitz and Newsome 1999; Kim and Shadlen 1999; Roitman and Shadlen 2002; Ding and Gold 2010). Neural correlates of the threshold crossing have been identified in LIP using the RT DOTS task (Roitman and Shadlen 2002).

The present results extend the earlier experimental results from FEF that used a fixed-duration version of the DOTS task by establishing a more precise correspondence between neuronal activity and decision formation over time (Kim and Shadlen 1999). In particular, we showed that a substantial subset of FEF neurons encode properties of the incoming stimulus and resulting choice in a manner consistent with the DDM-like decision process. On average, this activity builds up (for choices into a given neuron's RF) or down (for choices out of the neuron's RF) as a function of both motion strength and viewing time as the monkey was viewing the motion stimulus and forming the direction decision. This activity became increasingly selective for the behavioral choice during stimulus viewing, ultimately reaching a common, coherence-independent level just before the onset of the saccade to the preferred target.

This rise-to-threshold pattern of DDM-like activity is reminiscent of presaccadic activity in FEF movement neurons for countermanding and visual-search tasks (Hanes and Schall 1996; Bichot, Thompson, et al. 2001). For the countermanding task, the subject is required to occasionally withhold a planned saccadic eye movement to a clearly indicated visual target. For the visual-search task, the subject is required to identify a singleton of particular features in the presence of distractors. These conditions also give rise to variable RTs, which can be explained by a variable rate of rise of presaccadic FEF activity and then convergence to a common threshold, which triggers the saccades 200–300 ms after stimulus onset (Hanes and Schall 1996; Purcell et al. 2010).

Despite the similarities between neuronal activity in FEF and the DDM, several issues remain unresolved. For example, we do not know how saccade-related accumulation-to-bound processes are related to the slower, DOTS-related decision process that we measured. One possibility is that they are the same process, both reflecting a conversion of sensory input plus noise into a saccadic choice, with the accumulating, partial information continuously feeding into FEF activity (Gold and Shadlen 2000; Bichot, Chenchal, et al. 2001). However, the dynamics of this process likely depend on the specific task, as suggested by the fact that convergence times on our task were substantially longer than those previously estimated for other tasks (Becker and Jurgens 1979; Brown et al. 2008). Conversely, perceptual decision and saccade generation might be represented discretely in FEF, as suggested by different responses of FEF visual neurons and movement neurons on visual-search tasks (Woodman et al. 2008). Our observation of differences in convergence time suggests an additional dissociation between neurons with different waveforms. Neurons with narrow spikes, whose activity tends to converge much earlier than saccade onset, might represent the direction decision, whereas neurons with broad spikes, whose activity tends to converge just before saccade onset, might represent the saccade plan. By maintaining these 2 representations, FEF could help facilitate more flexible relationships between the perceptual decision from the corresponding action, for example, during learning of a new sensorimotor mapping or when a delay between the decision and action is desirable.

More generally, we do not have a complete account of all of the time typically taken from motion onset to the saccadic response on the DOTS task. Temporal integration times for this task tend to be substantially longer than for other perceptual tasks, lasting many hundreds of milliseconds even for well-trained human and monkey subjects (Smith 1998; Roitman and Shadlen 2002; Palmer et al. 2005; Hanks et al. 2006). The monkeys in the present study had particularly long RTs, possibly reflecting our overly successful efforts to train them out of their initial predispositions to respond too quickly. Despite a rough correspondence between the decision times predicted by our behavioral fits and the time course of DDM-like activity in FEF, we do not know the exact relationship between the two. For example, we found neural convergence times (i.e., the presumed end of the DDM-like decision process) that occurred ~150 ms before saccade onset, implying a long "postdecision" period. We do not know what the FEF responses are encoding during this time, including possibly continued deliberations (Resulaj et al. 2009) or simply a delay before the saccade is executed.

Finally, we also do not yet have a complete account of how and where in the brain nonsensory factors are incorporated into the decision process. For this kind of choice task, biased decision behavior is a frequent phenomenon for even well-trained human or monkey subjects (Green and Swets 1966). Biases can arise from different sources. One source is explicit manipulation of prior probabilities, which was recently shown to affect decision-related processing in LIP for the DOTS task (Hanks et al. 2011). Conversely, subjects can have idiosyncratic biases that do not necessarily reflect aspects of the task design, as was the case for the monkeys in this study, particularly monkey F. We recently reported neuronal correlates of this kind of idiosyncratic bias in caudate (Ding and Gold 2010). However, using the same analytical methods and the same animals as in that study, we did not observe similar bias-related activity in FEF. More work is needed to determine the relative roles of FEF, caudate, and other brain regions in processing prior probabilities and other types of internal factors (e.g., reward expectation, attention) that can bias decision-making behavior.

Decision-Trace Activity

Effective decision making requires ongoing calibration to ensure that goals are consistently met. Our finding of stimulus-related processing following decision commitment is consistent with an evaluative role that could service such calibration. It has been long known that a substantial proportion of FEF neurons show spatially selective postsaccadic activity (Bizzi 1968). However, such activity tended to be indifferent to task context (e.g., goal-directed vs. spontaneous saccades) or reward contingency (Goldberg and Bruce 1990; Roesch and Olson 2003; Ding and Hikosaka 2006). On the more perceptually demanding DOTS task, the activity of a large proportion of FEF neurons continues to be modulated by the choice just made and the motion strength of the stimulus that led to that choice. This activity provides a "memory trace" of the decision process, which could be used to compute evaluative quantities, such as reward prediction or choice uncertainty, well after the decision has been made but closer in time to the actual reward outcome.

We found that the decision-trace activity persisted after saccade onset and was present in a large proportion of FEF neurons on the DOTS task. In contrast, reward-modulated

activity in FEF occurs primarily before saccades and is observed much less frequently (Roesch and Olson 2003; Ding and Hikosaka 2006). The apparent timing difference might reflect the difference between prolonged decisions based on noisy motion inputs and immediate decisions after suprathreshold visual cues. The difference in frequency might reflect the challenge of estimating reward expectation from an accumulation of noisy evidence.

Response Heterogeneity in FEF

Our data showed that even within FEF there is substantial response heterogeneity. With the assumption that neurons with broad and narrow spikes correspond to excitatory and inhibitory neurons, respectively, our data provide the first characterization of inhibitory activity on a perceptual decision-making task and put new constraints on the neural implementation of the decision process. Inhibition has also been a critical component of many decision models. For example, surround suppression of FEF responses has been postulated to facilitate target selection in visual search by providing location-sensitive, but less feature-sensitive, inhibition to discourage distractor selection (Schall, Hanes, et al. 1995; Schall et al. 2004). Lateral inhibition between neurons with different preferred motion directions was necessary to keep activity from saturating in a Bayesian model using LIP as the evidence accumulator on DOTS tasks (Beck et al. 2008). Likewise, inhibition was used to implement competition between alternative choices in a leaky, competing accumulator model, although the neural population and connection patterns that might mediate such lateral inhibition was not specified (Usher and McClelland 2001). In a recurrent network simulating LIP activity, a set of interneurons that pooled activity from all excitatory neurons provided uniform feedback inhibition for a winner-take-all competition between alternative choices (Wang 2002; Furman and Wang 2008). Such uniform inhibition is in contrast to the choice- and coherence-modulated responses of narrow-spike FEF neurons in our study, although we do not know the number of nontask-modulated inhibitory FEF neurons that contribute to our task. In addition, one implied assumption common to these models is that the inhibitory activity derives directly from input from excitatory neurons, the latter performing the accumulation of evidence or similar computations. Our results showed that neurons with narrow spikes converged to a common level sooner than neurons with broad spikes, suggesting that inhibitory neurons play additional computational functions beyond merely tracking excitatory neurons. It will be important to examine further how these 2 neuron types interact, whether their responses are modulated differently by task or reward contexts, and how their interactions contribute to the final decisions.

Functional heterogeneity within FEF has also been traditionally documented using visual, visuomovement, and movement categories, defined using variations of the MGS task (Bruce and Goldberg 1985). Recent studies using visual-search and saccade-countermanding tasks have further emphasized distinct functions of these neuron groups (Woodman et al. 2008; Ray et al. 2009; Purcell et al. 2010). Neural activity on one of these tasks is highly predictive of the same neuron's response on the other tasks. In contrast, we found that activity could differ substantially between the MGS and DOTS tasks. For example, only a subset of neurons categorized as either VM or M on the MGS task demonstrate DDM-like or trace activity on the DOTS task. Likewise, only ~30% of neurons with delay-period activation on the MGS task showed DDM-like activity on the DOTS task, consistent with previous findings using a different variant of the motion-discrimination task (Kim and Shadlen 1999). Conversely, neurons of different traditional categories can show similar responses on the DOTS task, especially for VM and M neurons (Fig. 11), although these responses may serve different functions in generating, evaluating, or adjusting decisions (Gold and Shadlen 2007; Kiani and Shadlen 2009; Law and Gold 2009). The task dependence suggests that FEF neurons can participate in different neural computations on different tasks. Furthermore, it underscores the functional importance of cell type identity (e.g., inhibitory or excitatory), connectivity patterns among different categories, and input/output connections of FEF neurons.

Comparison of FEF, LIP, and Caudate

The correspondence between neural activity and an accumulate-to-bound process has been tested in 2 other brain regions, LIP and caudate, using the same RT DOTS task (Roitman and Shadlen 2002; Ding and Gold 2010). Similar analyses have also been applied to neural data from the SC for a fixed-duration version of the DOTS task and RT versions of other 2-choice visual tasks (Horwitz and Newsome 1999; Ratcliff et al. 2003, 2007). In all of these cases, activity in subsets of neurons reflects a gradual buildup of information that depends on both the strength of the stimulus and the final saccadic choice. Moreover, this buildup appears to reach a fixed bound in LIP and SC. Together, these results imply that these heavily interconnected oculomotor brain regions make strongly overlapping contributions to visuomotor decisions.

Nevertheless, differences in the timing and dynamics of activity from these different brain regions help illuminate their relative contributions. Because different task designs can affect how and where the decision process is represented in the brain, here, we make direct quantitative comparisons only for FEF, LIP, and caudate activity measured during the RT DOTS task. However, even these comparisons should not be taken as definitive: The LIP data were collected in a different lab than the FEF and caudate data, and although the FEF and caudate data came from the same monkeys, they were collected at different times.

DDM-like activity in FEF and LIP was similar during motion viewing. In particular, activity differentiated between the 2 choices ~200 ms after motion-stimulus onset, ramped up and down in a coherence-dependent manner for IN and OUT trials, respectively, and reached a common peak level ~100 ms before saccade onset on IN trials. The ratio of activity levels during motion viewing and saccade generation was comparable. The time of activity convergence in LIP was also within the range of that for neurons with broad spikes, but later than for neurons with narrow spikes, in FEF. With the assumed correspondence between broad spikes and pyramidal neurons in FEF (Shin and Sommer 2006) and given that both FEF and LIP receive inputs from MT and are reciprocally connected (Kunzle and Akert 1977; Barbas and Mesulam 1981; Petrides and Pandya 1984; Andersen et al. 1985; Huerta et al. 1987; Selemon and Goldman-Rakic 1988; Blatt et al. 1990; Felleman and Van Essen 1991; Schall, Morel, et al. 1995; Stanton et al. 1995; Tian and Lynch 1996), these results suggest that FEF and LIP play parallel roles during the accumulation-to-bound process.

DDM-like activity in FEF and LIP shares some common features with caudate activity, as well, including substantial choice and coherence dependence during motion viewing. However, in caudate, the emergence of choice dependence was earlier and the coherence dependence persisted even through the saccadic response. Thus, although caudate neurons receive direct projections from FEF and LIP, other brain regions likely contribute at least partly to the motion stimulus–driven activity in caudate. For example, motion-sensitive inputs might reach caudate from the dorsolateral PFC in an already decision-related form or from MT in a less processed form because both cortical areas project directly to caudate (Kemp and Powell 1970; Goldman and Nauta 1977; Yeterian and Van Hoesen 1978; Maunsell and van Essen 1983; Selemon and Goldman-Rakic 1985; Eblen and Graybiel 1995; Yeterian and Pandya 1995). In addition, the nonconverging activity pattern in caudate suggests that the cortical areas are more closely linked to decision commitment. Instead, caudate, perhaps in tandem with the decision-trace signals found in FEF, appears to monitor overall performance regardless of the identity of each choice and provide adjustment accordingly.

Thus, the accumulated quantity may be used differently in multiple brain areas to support complementary roles in decision making. In addition to FEF, LIP, and caudate, for visually guided oculomotor tasks like the one we used, these brain areas likely also include the SC, which plays a central role in saccade output, and parts of the medial PFC, which encode performance-monitoring signals for a variety of tasks (Stuphorn et al. 2000; Ito et al. 2003; Emeric et al. 2008, 2010). More work is needed to understand the specific contributions made by each of these different brain regions to particular tasks involving saccadic decisions.

Conclusions

In summary, we showed that single-neuron activity in FEF encodes both the transformation of incoming motion information into a categorical saccadic choice and the maintenance of that information after a decision was made. Given the abundance of reward and attentional modulation in FEF (Coe et al. 2002; Roesch and Olson 2003; Sato and Schall 2003; Thompson and Bichot 2005; Thompson, Biscoe, et al. 2005; Ding and Hikosaka 2006), our results suggest that FEF mediates a DDM-like decision-making process in parallel to LIP and provide additional decision-trace signals that, via interactions with the basal ganglia, can help to facilitate behavioral flexibility.

Supplementary Material

Supplementary material can be found at: http://www.cercor.oxfordjournals.org/

Funding

National Institutes of Health (K99EY018042 and American Recovery and Reinvestment Act of 2009 supplement to L.D.); McKnight Endowment Fund for Neuroscience; Sloan Foundation; Burroughs-Wellcome Fund (to J.I.G.).

Notes

We thank Rishi Kalwani for assistance with MR images; Benjamin Heasly for hardware and software support; Timothy Hanks and Michael Shadlen for assistance with the DDM; Jamie Roitman for advice on behavioral training; and Jean Zweigle for excellent animal care. *Conflict of Interest* : None declared.

References

Andersen RA, Asanuma C, Cowan WM. 1985. Callosal and prefrontal associational projecting cell populations in area 7A of the macaque monkey: a study using retrogradely transported fluorescent dyes. J Comp Neurol. 232:443–455.

Barbas H, Mesulam MM. 1981. Organization of afferent input to subdivisions of area 8 in the rhesus monkey. J Comp Neurol. 200:407–431.

Beck JM, Ma WJ, Kiani R, Hanks T, Churchland AK, Roitman J, Shadlen MN, Latham PE, Pouget A. 2008. Probabilistic population codes for Bayesian decision making. Neuron. 60:1142–1152.

Becker W, Jurgens R. 1979. An analysis of the saccadic system by means of double step stimuli. Vision Res. 19:967–983.

Bichot NP, Chenchal Rao S, Schall JD. 2001. Continuous processing in macaque frontal cortex during visual search. Neuropsychologia. 39:972–982.

Bichot NP, Schall JD. 1999. Saccade target selection in macaque during feature and conjunction visual search. Vis Neurosci. 16:81–89.

Bichot NP, Schall JD. 2002. Priming in macaque frontal cortex during popout visual search: feature-based facilitation and location-based inhibition of return. J Neurosci. 22:4675–4685.

Bichot NP, Thompson KG, Chenchal Rao S, Schall JD. 2001. Reliability of macaque frontal eye field neurons signaling saccade targets during visual search. J Neurosci. 21:713–725.

Bizzi E. 1968. Discharge of frontal eye field neurons during saccadic and following eye movements in unanesthetized monkeys. Exp Brain Res. 6:69–80.

Blatt GJ, Andersen RA, Stoner GR. 1990. Visual receptive field organization and cortico-cortical connections of the lateral intraparietal area (area LIP) in the macaque. J Comp Neurol. 299:421–445.

Boussaoud D, Ungerleider LG, Desimone R. 1990. Pathways for motion analysis: cortical connections of the medial superior temporal and fundus of the superior temporal visual areas in the macaque. J Comp Neurol. 296:462–495.

Brown JW, Hanes DP, Schall JD, Stuphorn V. 2008. Relation of frontal eye field activity to saccade initiation during a countermanding task. Exp Brain Res. 190:135–151.

Bruce CJ, Goldberg ME. 1985. Primate frontal eye fields. I. Single neurons discharging before saccades. J Neurophysiol. 53:603–635.

Bruce CJ, Goldberg ME, Bushnell MC, Stanton GB. 1985. Primate frontal eye fields. II. Physiological and anatomical correlates of electrically evoked eye movements. J Neurophysiol. 54:714–734.

Burman DD, Bruce CJ. 1997. Suppression of task-related saccades by electrical stimulation in the primate's frontal eye field. J Neurophysiol. 77:2252–2267.

Chen Y, Martinez-Conde S, Macknik SL, Bereshpolova Y, Swadlow HA, Alonso JM. 2008. Task difficulty modulates the activity of specific neuronal populations in primary visual cortex. Nat Neurosci. 11:974–982.

Coe B, Tomihara K, Matsuzawa M, Hikosaka O. 2002. Visual and anticipatory bias in three cortical eye fields of the monkey during an adaptive decision-making task. J Neurosci. 22:5081–5090.

Cohen JY, Heitz RP, Woodman GF, Schall JD. 2009. Neural basis of the set-size effect in frontal eye field: timing of attention during visual search. J Neurophysiol. 101:1699–1704.

Cohen JY, Pouget P, Heitz RP, Woodman GF, Schall JD. 2009. Biophysical support for functionally distinct cell types in the frontal eye field. J Neurophysiol. 101:912–916.

Constantinidis C, Goldman-Rakic PS. 2002. Correlated discharges among putative pyramidal neurons and interneurons in the primate prefrontal cortex. J Neurophysiol. 88:3487–3497.

Ding L, Gold JI. 2010. Caudate encodes multiple computations for perceptual decisions. J Neurosci. 30:15747–15759.

Ding L, Hikosaka O. 2006. Comparison of reward modulation in the frontal eye field and caudate of the macaque. J Neurosci. 26:6695–6703.

Ditterich J. 2006. Stochastic models of decisions about motion direction: behavior and physiology. Neural Netw. 19:981–1012.

Eblen F, Graybiel AM. 1995. Highly restricted origin of prefrontal cortical inputs to striosomes in the macaque monkey. J Neurosci. 15:5999–6013.
Emeric EE, Brown JW, Leslie M, Pouget P, Stuphorn V, Schall JD. 2008. Performance monitoring local field potentials in the medial frontal cortex of primates: anterior cingulate cortex. J Neurophysiol. 99:759–772.
Emeric EE, Leslie M, Pouget P, Schall JD. 2010. Performance monitoring local field potentials in the medial frontal cortex of primates: supplementary eye field. J Neurophysiol. 104:1523–1537.
Felleman DJ, Van Essen DC. 1991. Distributed hierarchical processing in the primate cerebral cortex. Cereb Cortex. 1:1–47.
Ferrera VP, Barborica A. 2010. Internally generated error signals in monkey frontal eye field during an inferred motion task. J Neurosci. 30:11612–11623.
Ferrera VP, Yanike M, Cassanello C. 2009. Frontal eye field neurons signal changes in decision criteria. Nat Neurosci. 12:1458–1462.
Furman M, Wang XJ. 2008. Similarity effect and optimal control of multiple-choice decision making. Neuron. 60:1153–1168.
Gold JI, Shadlen MN. 2000. Representation of a perceptual decision in developing oculomotor commands. Nature. 404:390–394.
Gold JI, Shadlen MN. 2002. Banburismus and the brain: decoding the relationship between sensory stimuli, decisions, and reward. Neuron. 36:299–308.
Gold JI, Shadlen MN. 2003. The influence of behavioral context on the representation of a perceptual decision in developing oculomotor commands. J Neurosci. 23:632–651.
Gold JI, Shadlen MN. 2007. The neural basis of decision making. Annu Rev Neurosci. 30:535–574.
Goldberg ME, Bruce CJ. 1990. Primate frontal eye fields. III. Maintenance of a spatially accurate saccade signal. J Neurophysiol. 64:489–508.
Goldman PS, Nauta WJ. 1977. An intricately patterned prefronto-caudate projection in the rhesus monkey. J Comp Neurol. 72:369–386.
Good IJ. 1979. Studies in the history of probability and statistics. XXXVII A.M. Turing's statistical work in World War II. Biometrika. 66:393–396.
Good IJ. 1983. Good thinking: the foundations of probability and its applications. Minneapolis (MN): University of Minnesota Press.
Green DM, Swets JA. 1966. Signal detection theory and psychophysics. New York: Wiley.
Grossberg S, Pilly PK. 2008. Temporal dynamics of decision-making during motion perception in the visual cortex. Vision Res. 48:1345–1373.
Hanes DP, Schall JD. 1996. Neural control of voluntary movement initiation. Science. 274:427–430.
Hanks TD, Ditterich J, Shadlen MN. 2006. Microstimulation of macaque area LIP affects decision-making in a motion discrimination task. Nat Neurosci. 9:682–689.
Hanks TD, Mazurek ME, Kiani R, Hopp E, Shadlen MN. 2011. Elapsed decision time affects the weighting of prior probability in a perceptual decision task. J Neurosci. 31:6339–6352.
Horwitz GD, Newsome WT. 1999. Separate signals for target selection and movement specification in the superior colliculus. Science. 284:1158–1161.
Huerta MF, Krubitzer LA, Kaas JH. 1987. Frontal eye field as defined by intracortical microstimulation in squirrel monkeys, owl monkeys, and macaque monkeys. II. Cortical connections. J Comp Neurol. 265:332–361.
Hussar CR, Pasternak T. 2009. Flexibility of sensory representations in prefrontal cortex depends on cell type. Neuron. 64:730–743.
Ito S, Stuphorn V, Brown JW, Schall JD. 2003. Performance monitoring by the anterior cingulate cortex during saccade countermanding. Science. 302:120–122.
Johnston K, DeSouza JF, Everling S. 2009. Monkey prefrontal cortical pyramidal and putative interneurons exhibit differential patterns of activity between prosaccade and antisaccade tasks. J Neurosci. 29:5516–5524.
Kemp JM, Powell TP. 1970. The cortico-striate projection in the monkey. Brain. 93:525–546.
Kiani R, Hanks TD, Shadlen MN. 2008. Bounded integration in parietal cortex underlies decisions even when viewing duration is dictated by the environment. J Neurosci. 28:3017–3029.
Kiani R, Shadlen MN. 2009. Representation of confidence associated with a decision by neurons in the parietal cortex. Science. 324:759–764.
Kim JN, Shadlen MN. 1999. Neural correlates of a decision in the dorsolateral prefrontal cortex of the macaque. Nat Neurosci. 2:176–185.
Klein SA. 2001. Measuring, estimating, and understanding the psychometric function: a commentary. Percept Psychophys. 63:1421–1455.
Kunzle H, Akert K. 1977. Efferent connections of cortical, area 8 (frontal eye field) in Macaca fascicularis. A reinvestigation using the autoradiographic technique. J Comp Neurol. 173:147–164.
Law CT, Gold JI. 2009. Reinforcement learning can account for associative and perceptual learning on a visual-decision task. Nat Neurosci. 12:655–663.
Maunsell JH, van Essen DC. 1983. The connections of the middle temporal visual area (MT) and their relationship to a cortical hierarchy in the macaque monkey. J Neurosci. 3:2563–2586.
Mazurek ME, Roitman JD, Ditterich J, Shadlen MN. 2003. A role for neural integrators in perceptual decision making. Cereb Cortex. 13:1257–1269.
Mitchell JF, Sundberg KA, Reynolds JH. 2007. Differential attention-dependent response modulation across cell classes in macaque visual area V4. Neuron. 55:131–141.
Monosov IE, Sheinberg DL, Thompson KG. 2010. Paired neuron recordings in the prefrontal and inferotemporal cortices reveal that spatial selection precedes object identification during visual search. Proc Natl Acad Sci U S A. 107:13105–13110.
Monosov IE, Thompson KG. 2009. Frontal eye field activity enhances object identification during covert visual search. J Neurophysiol. 102:3656–3672.
Moore T, Armstrong KM. 2003. Selective gating of visual signals by microstimulation of frontal cortex. Nature. 421:370–373.
Moore T, Fallah M. 2001. Control of eye movements and spatial attention. Proc Natl Acad Sci U S A. 98:1273–1276.
Newsome WT, Britten KH, Movshon JA. 1989. Neuronal correlates of a perceptual decision. Nature. 341:52–54.
Palmer J, Huk AC, Shadlen MN. 2005. The effect of stimulus strength on the speed and accuracy of a perceptual decision. J Vis. 5: 376–404.
Parker AJ, Newsome WT. 1998. Sense and the single neuron: probing the physiology of perception. Annu Rev Neurosci. 21:227–277.
Petrides M, Pandya DN. 1984. Projections to the frontal cortex from the posterior parietal region in the rhesus monkey. J Comp Neurol. 228:105–116.
Purcell BA, Heitz RP, Cohen JY, Schall JD, Logan GD, Palmeri TJ. 2010. Neurally constrained modeling of perceptual decision making. Psychol Rev. 117:1113–1143.
Rao SG, Williams GV, Goldman-Rakic PS. 1999. Isodirectional tuning of adjacent interneurons and pyramidal cells during working memory: evidence for microcolumnar organization in PFC. J Neurophysiol. 81:1903–1916.
Ratcliff R, Cherian A, Segraves M. 2003. A comparison of macaque behavior and superior colliculus neuronal activity to predictions from models of two-choice decisions. J Neurophysiol. 90:1392–1407.
Ratcliff R, Hasegawa YT, Hasegawa RP, Smith PL, Segraves MA. 2007. Dual diffusion model for single-cell recording data from the superior colliculus in a brightness-discrimination task. J Neurophysiol. 97:1756–1774.
Ratcliff R, Rouder JN. 1998. Modeling response times for two-choice decisions. Psychol Sci. 9:347–356.
Ratcliff R, Smith PL. 2004. A comparison of sequential sampling models for two-choice reaction time. Psychol Rev. 111:333–367.
Ray S, Pouget P, Schall JD. 2009. Functional distinction between visuomovement and movement neurons in macaque frontal eye field during saccade countermanding. J Neurophysiol. 102:3091–3100.
Resulaj A, Kiani R, Wolpert DM, Shadlen MN. 2009. Changes of mind in decision-making. J Nature. 461:263–266.
Robinson DA, Fuchs AF. 1969. Eye movements evoked by stimulation of frontal eye fields. J Neurophysiol. 32:637–648.
Roesch MR, Olson CR. 2003. Impact of expected reward on neuronal activity in prefrontal cortex, frontal and supplementary eye fields and premotor cortex. J Neurophysiol. 90:1766–1789.

Roitman JD, Shadlen MN. 2002. Response of neurons in the lateral intraparietal area during a combined visual discrimination reaction time task. J Neurosci. 22:9475–9489.
Sato T, Schall JD. 2001. Pre-excitatory pause in frontal eye field responses. Exp Brain Res. 139:53–58.
Sato TR, Schall JD. 2003. Effects of stimulus-response compatibility on neural selection in frontal eye field. Neuron. 38:637–648.
Schall JD, Hanes DP, Thompson KG, King DJ. 1995. Saccade target selection in frontal eye field of macaque. I. Visual and premovement activation. J Neurosci. 15:6905–6918.
Schall JD, Morel A, King DJ, Bullier J. 1995. Topography of visual cortex connections with frontal eye field in macaque: convergence and segregation of processing streams. J Neurosci. 15:4464–4487.
Schall JD, Sato TR, Thompson KG, Vaughn AA, Juan CH. 2004. Effects of search efficiency on surround suppression during visual selection in frontal eye field. J Neurophysiol. 91:2765–2769.
Schiller PH, True SD, Conway JL. 1979. Effects of frontal eye field and superior colliculus ablations on eye movements. Science. 206:590–592.
Selemon LD, Goldman-Rakic PS. 1985. Longitudinal topography and interdigitation of corticostriatal projections in the rhesus monkey. J Neurosci. 5:776–794.
Selemon LD, Goldman-Rakic PS. 1988. Common cortical and subcortical targets of the dorsolateral prefrontal and posterior parietal cortices in the rhesus monkey: evidence for a distributed neural network subserving spatially guided behavior. J Neurosci. 8:4049–4068.
Shadlen MN, Hanks TD, Churchland AK, Kiani R, Yang T. 2006. The speed and accuracy of a simple perceptual decision: a mathematical primer. In: Doya K, Ishii S, Rao R, Pouget A, editors. Bayesian brain: probabilistic approaches to neural coding. Cambridge (MA): MIT Press.
Shadlen MN, Newsome WT. 1996. Motion perception: seeing and deciding. Proc Natl Acad Sci U S A. 93:628–633.
Shadlen MN, Newsome WT. 2001. Neural basis of a perceptual decision in the parietal cortex (area LIP) of the rhesus monkey. J Neurophysiol. 86:1916–1936.
Shin SY, Sommer MA. 2006. Frontal eye field input neurons have higher spontaneous firing rates and narrower action potentials than output neurons. J Soc Neurosci Abstr. 138:111.
Smith PL. 1998. Bloch's law predictions from diffusion process models of detection. Aust J Psychol. 50:139–147.
Smith PL, Ratcliff R. 2004. Psychology and neurobiology of simple decisions. Trends Neurosci. 27:161–168.
Song JH, McPeek RM. 2010. Roles of narrow- and broad-spiking dorsal premotor area neurons in reach target selection and movement production. J Neurophysiol.
Stanton GB, Bruce CJ, Goldberg ME. 1995. Topography of projections to posterior cortical areas from the macaque frontal eye fields. J Comp Neurol. 353:291–305.
Stuphorn V, Taylor TL, Schall JD. 2000. Performance monitoring by the supplementary eye field. Nature. 408:857–860.
Tamura H, Kaneko H, Kawasaki K, Fujita I. 2004. Presumed inhibitory neurons in the macaque inferior temporal cortex: visual response properties and functional interactions with adjacent neurons. J Neurophysiol. 91:2782–2796.
Thompson KG, Bichot NP. 2005. A visual salience map in the primate frontal eye field. Prog Brain Res. 147:251–262.
Thompson KG, Bichot NP, Sato TR. 2005. Frontal eye field activity before visual search errors reveals the integration of bottom-up and top-down salience. J Neurophysiol. 93:337–351.
Thompson KG, Biscoe KL, Sato TR. 2005. Neuronal basis of covert spatial attention in the frontal eye field. J Neurosci. 25:9479–9487.
Thompson KG, Hanes DP, Bichot NP, Schall JD. 1996. Perceptual and motor processing stages identified in the activity of macaque frontal eye field neurons during visual search. J Neurophysiol. 76:4040–4055.
Tian JR, Lynch JC. 1996. Corticocortical input to the smooth and saccadic eye movement subregions of the frontal eye field in Cebus monkeys. J Neurophysiol. 76:2754–2771.
Trageser JC, Monosov IE, Zhou Y, Thompson KG. 2008. A perceptual representation in the frontal eye field during covert visual search that is more reliable than the behavioral report. Eur J Neurosci. 28:2542–2549.
Usher M, McClelland JL. 2001. The time course of perceptual choice: the leaky, competing accumulator model. Psychol Rev. 108:550–592.
Wald A, Wolfowitz J. 1948. Optimum character of the sequential probability ratio test. Ann Math Stat. 19:326–339.
Wang XJ. 2002. Probabilistic decision making by slow reverberation in cortical circuits. Neuron. 36:955–968.
Wilson FA, O'Scalaidhe SP, Goldman-Rakic PS. 1994. Functional synergism between putative gamma-aminobutyrate-containing neurons and pyramidal neurons in prefrontal cortex. Proc Natl Acad Sci U S A. 91:4009–4013.
Wong KF, Wang XJ. 2006. A recurrent network mechanism of time integration in perceptual decisions. J Neurosci. 26:1314–1328.
Woodman GF, Kang MS, Thompson K, Schall JD. 2008. The effect of visual search efficiency on response preparation: neurophysiological evidence for discrete flow. Psychol Sci. 19:128–136.
Xiao Q, Barborica A, Ferrera VP. 2006. Radial motion bias in macaque frontal eye field. Vis Neurosci. 23:49–60.
Yeterian EH, Pandya DN. 1995. Corticostriatal connections of extrastriate visual areas in rhesus monkeys. J Comp Neurol. 352:436–457.
Yeterian EH, Van Hoesen GW. 1978. Cortico-striate projections in the rhesus monkey: the organization of certain cortico-caudate connections. Brain Res. 139:43–63.
Zhou HH, Thompson KG. 2009. Cognitively directed spatial selection in the frontal eye field in anticipation of visual stimuli to be discriminated. Vision Res. 49:1205–1215.